Workshop On 2-D Transport

February 1979

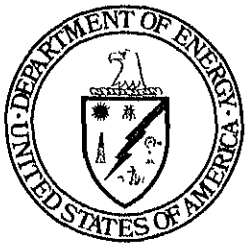

U.S. Department of Energy
Assistant Secretary for Energy
Office of Fusion Energy
Division of Applied Plasma Physics
Washington, D.C. 20545

Available from:

National Technical Information Service (NTIS)
U.S. Department of Commerce
5285 Port Royal Road
Springfield, Virginia 22161

Price: Printed Copy: $ 6.00
Microfiche: $ 3.00

WORKSHOP ON 2-D TRANSPORT

CORNELL UNIVERSITY

AUGUST 1978

PARTICIPANTS OF THE 2-D TRANSPORT WORKSHOP

AUGUST 1978

T. Antonsen, Massachusetts Institute of Technology
C. Boley, Argonne National Laboratory
A. Boozer, Princeton Plasma Physics Laboratory
D. Düchs, Max Planck Institute
H. Grad, New York University
F. Hinton, University of Texas
S. Hirshman, Oak Ridge National Laboratory
J. Hogan, Oak Ridge National Laboratory
P. Hu, New York University
S. Jardin, Princeton Plasma Physics Laboratory
D. Nelson, Oak Ridge National Laboratory
E. Ott, Cornell University
D. Post, Princeton Plasma Physics Laboratory
D. Stevens, New York University
C. Wagner, Science Applications, Incorporated
R. Waltz, General Atomic Company

W. Sadowski, Workshop Chairman, Department of Energy

TABLE OF CONTENTS

I. Introduction

Transport, along with such processes as radiation and wall recycling, determine the energy and particle confinement times as well as density and temperature profiles for ions and electrons. As a result, transport and atomic processes determine whether a particular equilibrium is accessible and how it will evolve. Transport predicts how energy and particle confinement times scale with average density, gross energy, radius, and temperature of the plasma. These so-called scaling laws are an important guide for the design of new confinement devices.

Transport codes are one of the essential research tools with which experimental data can be interpreted and theoretical ideas can be quantitatively tested. They isolate the role of various processes involved in transport. As an illustration, on the next page Fig. 1 shows the relative importance of the anomalous electron heat and plasma transport when the neoclassical heat transport is switched off. At the present time transport codes are much more useful as research tools than as predictive, reliable engineering design tools. This is because the transport rates are such as not to make the codes predictive. As a result, many of the major codes are not of completely general utility but have been developed with special emphasis on particular in-house experimental needs. This is no reflection on the effectiveness of the codes since simple treatments are quite often adequate. An example of

a research code which was designed, among other things, to test the range of validity of Pfirsch-Schluter diffusion is given in Appendix III.

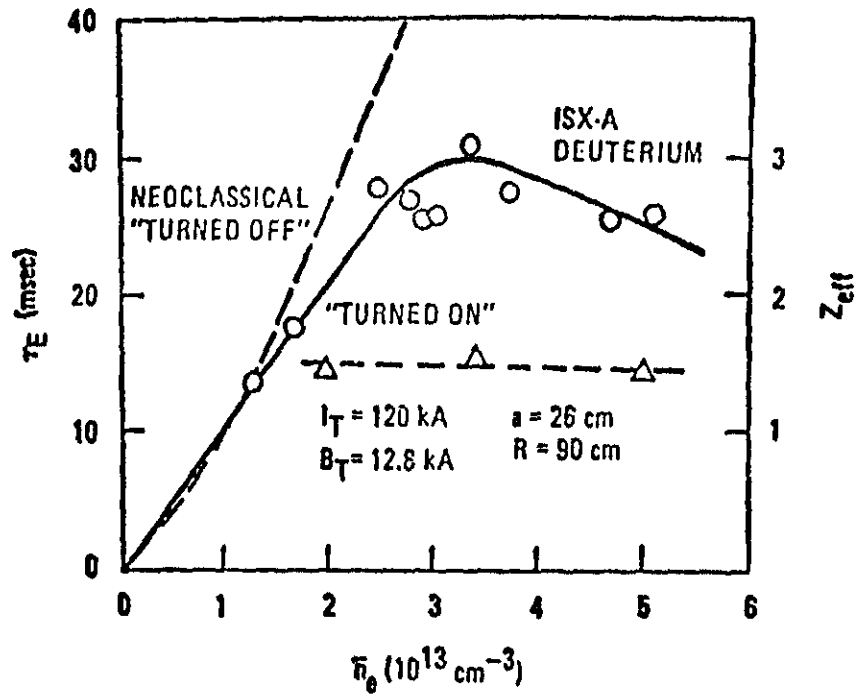

FIG. 1.* Density dependence of total energy confinement time for deuterium discharges in ISX-A with I = 120 kA and B_t = 12.8 kG. The solid line shows full transport model predictions, fit to the experimental point at $\bar{n} = 1.5 \times 10^{13}$ cm^{-3}. The dashed line shows the corresponding results with ion neoclassical thermal conductivity neglected in the transport model.

*R. E. Waltz and G. E. Guest, GA-A15048, to be published.

II. Summary

A workshop on 1-D and 2-D transport in tokamaks was held at Ithaca, New York on August 2-4, 1978. The purpose of the Workshop was to assess the status of physical models used in transport calculations and to evaluate the maturity of 2-D transport codes in predicting operating parameters of such confinement devices as Alcator, PLT, Doublet III, and TFTR.

The Workshop consisted of in-depth discussions of the following topics:

Status of 1-D codes, problems where 2-D treatment is necessary or useful, status of the treatment of fundamental processes, successful models, boundary and wall effects, 3-D and velocity space effects, and numerical algorithms used in transport codes.

Below is a brief summary of some of the discussions and conclusions:

Transport Modules. Since transport of ionized species along field lines is much faster than across field lines, transport in two and even three dimensions can be reduced to a one-dimensional problem dealing with transport across flux surfaces. Both 1-D and 2-D, or so-called 1½-D transport modules calculate radial, i.e., one-dimensional transport. The difference between the two classes of codes lies in how they treat the coupling between flux surface motion and conservation of mass, momentum, and flux.

1-D Codes. The surfaces of constant poloidal flux are assumed to be concentric toroids of circular cross section. The fact that experimental profiles are roughly symmetric justifies this assumption. It is important to emphasize that existing 1-D codes may contain a great deal of 2-D and 3-D information. For example, neutral beam deposition is calculated on the basis of 2-D particle orbits, fast ions are calculated on the basis of three velocity variables, flux surface averages are based on 2-D flux surfaces. All of this information is folded as coefficients into a differential equation that depends on radius and time only.

2-D Codes. Even though the transport module is 1-D, these codes solve fully 2-D problems to determine magnetic flux surfaces. Flux surface averages are performed on 2-D flux surfaces whose shape can change as a result of transport.

2-D codes must be used when there are moderate changes in magnetic geometry, for the design of magnetic circuitry, in MHD stability studies and ion beam deposition studies. It must be emphasized that the efficient use of 2-D codes increases CPU time by only 50%.

Physics Models. It was agreed that the models dealing with atomic processes and neutral particles are well in hand. Non-coronal models are available but are not yet in general use.

beam deposition, alpha particle heating, plasma

compression, and general gross 2-D motion of magnetic flux surfaces have reached advanced stages of development.

The physical boundary region of the plasma is not understood quantitatively. This includes production and inward transport of recycled material, partition of energy flow between wall and limiter, and non-coronal radiation from impurities.

There is little quantitative understanding of the anomalous electron heat and plasma transport. The simplest phenomenological approach has been to assign a value to the anomalous heat conductivity inversely proportional to the density. This gives the Alcator scaling, but the variation of conductivity by a factor of 3 to 5 from machine to machine has not been correlated with any systematic dependence.

More work needs to be done on anisotropic and other types of distortion of plasma equilibrium by neutral beam injection.

Future Directions

The development of transport codes will be affected by the amount and quality of experimental data available.

In the near future the codes will undergo improvements that will include the coupling of large impurity diffusion calculations to transport codes, and development of 3-D neutrals models to calculate effects of gas puffing. The coupling of MHD stability codes with transport calculations

will give information on the accessibility of high-beta states and on the effect of ballooning modes in these states. This area of research will receive increased emphasis at each major laboratory.

As the use of more physics and of higher spatial and velocity dimensions increases in the future, the codes will become more specialized to particular problems or machines. At the same time, development of large complex "master" codes will continue. These will be primarily used to check the output of the more specialized codes.

III. Recommendations

The Workshop participants have identified two areas that need particular attention. These are the lack of an experimental tokamak data base and the unavailability of neoclassical transport coefficients for arbitrary collisionality, geometry, and aspect ratio.

A. It is recommended that a Committee on the Tokamak Data Base be established to develop procedures by which properly aged data on tokamak experiments be made available to code builders. The Committee should consist predominantly of experimentalists, with a participation of theoreticians working in the field of transport.

B. It is recommended that a compendium of transport coefficients be made available in the parameter regions where they are understood. It is also recommended that encouragement be given to develop formulas for coefficients in parameter regions where they are not so well understood. For example, work should be encouraged on such things as neoclassical ion thermal conductivity and trapped particle corrections to the Ohm's law resistivity.

IV. Physical Models in Transport Codes

In order to calculate transport in a fusion device, a code must contain modules dealing with transport of several plasma species, anomalous effects, the effect of impurities, radiation losses, neutral injection, adiabatic compression, alpha particle heating, and plasma-wall and plasma-limiter interaction. The code must be such as to ensure particle and energy balance. Below we will discuss briefly each of these effects.

Plasma Species. In order to know profiles in a plasma, it is necessary to know how each species diffuses across the magnetic field. Consequently, transport codes treat more than one species of particles and more than one charge state of each species.

Anomalous Transport. In addition to classical transport due to Coulomb collisions and electric and magnetic field inhomogeneities, a plasma may diffuse across magnetic field lines due to various types of collective instabilities that are largely unrelated to classical transport. Such transport is called anomalous and for electrons it is in general higher than classical transport. A discussion of the problems in calculating anomalous transport is given in Section VI.

Impurity Effects and Radiative Losses. Impurities affect tokamaks by
na energy, contributing to Z_{eff} and thus increasing the ohmic
te, and by diluting the plasma. The calculation of impurity
s made great progress in the last few years. Atomic rates

for computing the impurity radiation power losses have been calculated for essentially all the known elements. The most common approximation used is to assume "coronal equilibrium" (ionization and recombination times short compared to diffusion times). This approximation is reasonably good for high Z elements (Z > 70), especially near the center of a tokamak. It is convenient since the power radiated can be computed from a simple formula $P_z = n_e n_z L_z(Te)$ where P_z is the power radiated in watts/cm^3, n_e is the electron density, n_z is the impurity density, and $L_z(Te)$ is the luminosity of the element which is a function of the electron temperature. Tables of fits to $L_z(Te)$ have been compiled and are used in most transport codes.

Coronal equilibrium is not a good approximation for low Z elements in devices with T_e > 200 eV. In these machines, the low Z impurities recycle at the edge. For example, oxygen ions enter as nearly neutral O^{+1}, etc., and are ionized rapidly to O^{+6}, and eventually to O^{+7} and O^{+8}. The partially ionized ions radiate furiously while they are being ionized. A single oxygen ion may radiate as much as 10 keV while being ionized (compared to $\sim$ 400 eV for the sum of ionization potentials for O^{+0} to O^{+6}). Once ionized the O^{+8} migrates into the center and comes out again, persisting almost to the limiter or wall, where it recombines and recycles again.

Models for this radiation have been constructed and used in some transport codes, but are not in common usage today.

Neutral Injection. As the beam particles penetrate the plasma, they undergo charge exchange with plasma ions and become ionized. In order to calculate the deposition of energy by neutral beam during injection beam ion trajectories must be obtained. These are obtained either by numerical integration of the standard guiding center equations for a torus or by calculating the effect of Coulomb collisions through the use of the Fokker-Planck equation. Neutral injection codes must be able to calculate deposition not only by full energy but also by 1/2 and 1/3 energy components of the beam.

Neutral Transport. Since particle confinement times in tokamaks are much shorter than the average pulse length, particle sources are important. The model used in calculations assumes that plasma diffuses out to the limiter and is neutralized. It recycles into the discharge as neutral gas which is ionized to form density sources. The neutral gas atoms can charge exchange with the plasma ions, and thus penetrate quite far into the plasma. Other sources of neutral gas beside recycling plasma are gas puffing, recombination, and neutral beam deposition.

Neutral gas transport is calculated from the linear Boltzmann equation. Semi-analytic slab models, discrete ordinate techniques, and Monte Carlo methods have been employed in the neutral gas problem.

Adiabatic Compression. The magnetic moment μ of a charged particle is invariant in a slowly varying magnetic field. As the field varies

in time, the Larmor orbits expand or contract and the charged particles lose or gain transverse energy through change in velocity and angular momentum perpendicular to the magnetic field. This transfer of energy between particles and the field can be used for plasma heating, known as adiabatic compression. Since devices like TFTR include adiabatic compression in their design, transport codes used to predict TFTR's performance must contain the compression module.

Alpha Particle Heating. An ignition reactor will be heated by alpha particles. Alpha particles are produced in the core of the reactor (50% of the α-energy is produced in 25% of the reactor radius). In order to determine the effect of α-particle heating, trajectories, confinement, loss cone, and slowing down mechanism for α-particles must be calculated. Determination of how α-particles diffuse and deposit their energy will affect temperature profiles of a reactor plasma. For example, if α-particles exhibit anomalous behavior due to instabilities, they will diffuse outward and will exhibit enhanced slowing down and a flatter temperature profile will result.

The modeling of classical alpha particle transport is in good shape. The effects of anomalous α-particle transport are not well understood. Theoretical studies in this area will receive increased emphasis as tokamak temperature increase.

Plasma-Wall and Plasma-Limiter Interaction. Impurities produce radiation losses in plasma. Heavy impurities have led to hollow temperature

profiles due to large radiation losses. Temperature and thickness of the cold plasma layer near the wall are important in predicting impurity recycling rates and charge exchange processes. Particle and energy fluxes to the limiter and the walls depend among other things on the temperature distribution in the plasma column, impurity species, impurity density, density gradients, and microinstabilities. Impurity production and transport are an important part of calculating confinement times in fusion devices. At present, impurities are treated by prescribing a source for impurities based on estimates of impurity production. With higher temperatures and densities, heat loads on the walls and the limiter may lead to enhanced impurity production. This will have a major effect on the operation of a fusion device. The area of plasma-wall and plasma-limiter interaction has not been receiving sufficient attention in the past. Theoretical efforts exist and new studies are being initiated but more attention is necessary.

V. Recent Developments in Transport Codes

The transport codes have been in a state of limbo for the past several years while the neutral injection tests were prepared. Concerning 1-D transport codes it was noted in 1975 that

> "Many models have been proposed to fit the data, and prompt the observation that these codes have reached maturity. Their adequacy can be tested against new experiments in new regimes, and further improvements may require a deeper treatment of the underlying physics."

With respect to prospects for further development of transport calculations, it was noted that

> "...the future prospects for transport code development seem to be along the lines of multi-dimensional calculations in physical and velocity space. When considering the upgrading of geometry (two dimensional), beams (Fokker-Planck equation), impurities (many data files for all species), neutrals (neutron transport codes), and plasma transport (instability simulation), it can be seen that complexity can grow easily."

In the interim period, development along the lines indicated above has occurred. There are now several 2-D transport codes, as well as two new efforts at ab initio calculation of transport rates (Grad-Nelson, Jardin-Hirshman) in 2-D geometry. There are also several Fokker-Planck transport codes and one code which does both 2-D and Fokker-Planck (to simulate TFTR injection/compression scenarios). Impurity radiation data files have been prepared for a substantial portion of the periodic

Table of the Elements, and impurity diffusion codes dealing with the simultaneous interaction of many charge states are now running. Monte Carlo and S_n treatments of neutral gas evolution have been developed as transport code modules. Multi-dimensional calculations of the sawtooth (m=1) MHD instability and of the saturation of m > 1 instabilities to form helical islands have been reduced to prescription form for inclusion in 1-D codes. Detailed comparison with experiment is underway, and will serve as a reference point for new results expected at high β_T.

From the above, one can see that the code development has proceeded in the predicted direction. The codes have now been tested against new experiments in new regimes: the recent PLT neutral beam injection results have proven out predictions of the neoclassical ion confinement model long used in transport calculations. While overall energy confinement is regarded as "anomalous," there have been new developments in calculation and measurement of high Z radiative effects and in the analysis of the role of large scale MHD islands on transport. Behavior previously seen as anomalous has subsequently been found to be dominated by radiation and/or MHD effects in some experiments. Since these processes can be modeled, there now exists a realistic prospect of resolving all anomalies.

Future Directions

With the clear endorsement provided by recent experimental results, transport code workers now have the responsibility to create accurate

computational models with less regard for computational size or complexity. There is a new generation of high beta, non-circular, and divertor tokamaks which will begin operation soon, and the understandable features of low β_T, circular plasmas must be computed as accurately as possible to serve as a reference. (The plasma near the magnetic axis will be stable to ballooning modes, have large-aspect ratio, and be approximately circular). Some examples of such computational improvements include coupling large impurity diffusion calculations to transport codes, providing 3-D neutrals modules to calculate jet effects of gas puffing and of neutral beam sources on toroidal average neutral density. The coupling of MHD instability codes with transport calculations will also be useful in computing the effects of ergodicity when many modes are present and to calculate the effects of ballooning instabilities at high beta. Fully 2-D codes are essential in understanding the dynamic interaction between realistic transport-induced pressure and current profiles, and experimental shape control and MHD stability. This area of research, namely the use of 2-D transport codes in conjunction with MHD ballooning codes, will receive increased emphasis at each of the major laboratories.

As the use of more physics and higher spatial and velocity dimensions increases in the future, codes will become increasingly specialized to particular problems or machines, e.g., doublets, divertor tokamaks, etc. Through specialization, these codes will permit more efficient use of computational resources and will provide more detailed answers to

specific problems. On the other hand, development will continue on sophisticated and complex codes that will contain a large number of physics modules and will be used primarily to check the output of more specialized codes in order to validate the assumptions made. To take an example from the present use of this technique, 2-D codes which follow the detailed time-dependent motion of the magnetic flux surfaces are not necessary to adequately calculate loss of confinement due to collisions and microinstabilities. Simple "fixed shape" approximations (even simple unphysical shapes such as ellipses) are more than adequate.

The development of codes will be affected by the amount and quality of experimental data available to them. A more detailed discussion of this problem is given in the section on "Tokamak Data Reporting."

VI. Present Status of Physics Models

There is a general consensus among workers in the field that some phenomena contributing to transport are well understood while others are not. Basically many areas dealing with atomic physics and neutrals are well in hand, but production and inward transport of recycled material is still poorly understood. Calculations for neutral beam deposition, alpha particle heating, plasma compression, and general gross 2-D motion of the magnetic flux surfaces have reached advanced stages of development.

The physical boundary region of the plasma is not understood quantitatively. The partition of energy flow between wall and limiter depends on a detailed knowledge of the transport coefficients as well as non-coronal radiation from impurities. On the other hand, the source of the impurities depends on the partitioned energy flux and detailed knowledge of irreproducible surfaces.* Semi-quantitative understanding of wall reflux physics is important to reactor studies and long-pulse tokamak operation. For this a "systems approach" rather than a partial differential equation approach may be most appropriate.

There is little understanding of the anomalous electron heat and plasma transport. This is due in part to the fact that experimental information from ohmically heated machines does not give a clear determination of

---

*Since it is not possible to exactly reproduce the condition of the walls and limiter from one shot to the next, we call these irreproducible surfaces.

the temperature dependence of the transport loss. Strong beam heating or a drastic radiation cooling of an ohmic discharge with a direct measurement of the conduction is required for this determination. Since temperatures from ohmically heated clean discharges are correlated with current and size for example, the absolute dependence on these variables cannot be determined without the knowledge of the temperature dependence. The simplest phenomenological description of anomalous transport is simply to assign a value to the anomalous conductivity proportional to 1/n. This gives Alcator density scaling. However, the value of the conductivity is not truly universal and a factor of 3 to 5 variation from machine to machine has not been successfully correlated with any systematic dependence. It should be clear that such imprecision of experimental knowledge allows a number of crude theoretical models (with one or more adjustable coefficients) to claim consistency with a large part of the data.

A major area of physics which has been studied for 2-D transport is the possible distortion of the plasma equilibrium by high-power neutral beam injection. In addition to heating and the formation of a high-energy tail in the ion-distribution function, high power neutral beam injection produces a toroidal current that affects the flux surfaces. The highly anisotropic spin-up of the plasma column also contributes to anisotropic pressure distribution ($P_{\parallel} \neq P_{\perp}$). The distortion of the flux surfaces due to pressure anisotropy can be handled with the generalized version of the Grad-Shafranov equation. None of the existing 2-D transport

codes can handle anisotropy or spin-up. The effect of anisotropic pressure should be comparable to the distortion of the surfaces from circular by the finite plasma pressure. The anisotropic pressure also implies a density variation along the flux surfaces of the order of the inverse aspect ratio. This density variation invalidates the usual argument for reducing the full 2-D transport problem to a 1-D flux surface averaged calculation. Due to great complexity of doing the problem correctly, the density variation effect on the transport may have to be ignored.

A. 2-D Transport: Why and How

A two-dimensional (2-D) configuration is defined to be one in which the flux function $\psi(x,z)$ (magnetic surfaces are defined by ψ = constant) depends on both the radial and vertical cylindrical coordinates (x,z). The concept of 2-D becomes particularly important when the surfaces change shape in time. The increased interest in low aspect ratio, non-circular cross section finite beta tokamaks calls for the two-dimensional treatment of flux surfaces. Among the practical situations where geometry and finite beta can markedly alter transport rates and energy balance, are adiabatic compression, magnetic axis shift and its effects on neutral beam penetration, surface shaping to reduce MHD instabilities, pc divertors, rapid FCT heating, and low aspect ratio devices

Since transport of ionized species (as opposed to neutrals lines is usually much faster than across field lines, tr or even three dimensions can be reduced to a one-dimensiona

dealing with transport across flux surfaces, augmented by a single 2-D equation describing the shape of flux surfaces. This approach has been called 1½-D. Self-consistent 1½-D transport calculations in which the transport processes (flows and surface-averaged transport rates) are computed self-consistently with the evolving surface shapes and magnetic field are necessary to obtain realistic pressure and magnetic field profiles to be used in magnetohydrodynamic stability calculations. The 1½-D description is valid for slow transport processes and excludes tearing modes, ballooning instabilities, and other fast processes that may remain inherently three-dimensional.

There are at least two reasons for requiring two-dimensional rather than one-dimensional treatment of plasma transport. First, the 2-D (non-circular) geometry of the flux surfaces modifies the value of the plasma transport coefficients. The resistive transport coefficients for diffusion normal to magnetic surfaces involve surface averages of various magnetic field quantities which are sensitive to the variation of $|\underset{\sim}{B}|$ along $\underset{\sim}{B}$. Thus, in high-β equilibria, where $|\underset{\sim}{B}|$ contours tend to align with the magnetic field, the neoclassical transport coefficients, as well as anomalous coefficients driven by magnetically trapped particles, could be substantially reduced from their usual 1-D values. For example, the vertical elongation of the plasma cross section increases neoclassical confinement time by decreasing the transport coefficients below the circular value by the square of the ellipticity.

Secondly, knowledge of the two-dimensional configuration of the plasma is necessary to apply boundary conditions and to compute the effects on the plasma of externally maintained heat and particle sources. Magnetic boundary conditions must be ultimately related to the currents in the poloidal field coils, whose spatial distribution is inherently two dimensional. The location of pressure contours, which approximately correspond to density contours, is important to determine heating and particle deposition profiles due to neutral beam injection.

There are various degrees of complexity in the formulation of the 1½-D transport problem. In the simplest 1½-D technique the flux surface shapes are assumed to be known and fixed in time and area weighting of transport coefficients is used in standard 1-D transport equations. This method is often used for low beta plasma with fixed surfaces. Unfortunately, it is not known whether simple area weighting correctly reflects the change in transport rates due to surface shaping especially for the empirical models used to describe the electron dynamics. In general, for reasonable surface shapes and parameters confinement times calculated with this formulation will be within a factor of two of those given by a 1-D cylinder model.

An intermediate technique goes beyond simply postulating the effects of geometry, but does not entail computing the complete transport flow problem. In this approach the surface-averaged fluxes are assumed to be known or postulated (from neoclassical theory or from a specific

model for anomalous transport) and they are used to calculate the change in plasma variables due to transport across surfaces of constant toroidal flux. As the plasma variables evolve, the 2-D (Grad-Shafranov) equation is solved numerically to obtain the shape of flux surfaces. This new geometric information is passed to the transport equations.

At present, the neoclassical transport coefficients needed to use this technique are not available in all collisionality regimes for arbitrary aspect ratio, arbitrary cross section or arbitrary β. The near axis(es) region of low aspect ratio non-circular finite β tokamaks may be adequately described with present theory, since the aspect ratio there is large, the surfaces may be nearly circular and this region most stable to ballooning. However, volume averaged β is the parameter of interest, and this depends on global knowledge of the transport rates.

Within the limitations of this model, however, there are experimental situations which it describes adequately. For example, the recent PLT neutral beam experiments employed a low n_e, high T_e target plasma to produce high proton temperatures. In this case the ion and electron energy balances were decoupled (by low n_e) and the injection energy went predominantly to the ions (high T_e, $E_{crit} \geq E_{injection}$). Adiabatic compression is another example where this approach is adequate, since the compression power supplies are chosen so that $\tau_{compression} << \tau_{energy}$. Injection and compression coupled together are also well treated, since the fast ion processes seem to be well described at present.

In the most sophisticated formulation of 1½-D transport, the transport processes (flows and surface averaged transport rates) are computed self-consistently with the evolving surface shapes and magnetic field. As was mentioned before, the self-consistent 1½-D transport calculations are necessary to obtain realistic pressure and magnetic field profiles to be used in magnetohydrodynamic stability calculations. Once a stable initial equilibrium configuration is specified, the time-dependent transport equations determine how that equilibrium evolves in time. In particular, if the time-dependent equations lead to a steady state, this corresponds to a unique prescription for the equilibrium profiles. The importance of these resistive steady states in determining unique stationary profiles of the otherwise arbitrary pressure and toroidal magnetic field functions $p(\psi)$ and $F(\psi)$ has been previously emphasized in publications.

Furthermore, a self-consistent 2-D calculation includes potentially important inductive contributions to the flux surface-averaged normal plasma flow arising from $\partial \underset{\sim}{B}/\partial t$. The maintenance of the lowest order (in resistivity η) pressure balance $\nabla p = \underset{\sim}{J} \times \underset{\sim}{B}$ on the resistive time scale can lead to deformations of the plasma magnetic surfaces, with associated self-consistent inductive $\underset{\sim}{E}^{(A)} \times \underset{\sim}{B}$ flows ($\underset{\sim}{E}^{(A)} = -\partial A/\partial t$) frequently greater than the resistive diffusion during the fast transient phase of the discharge. This inductive convection of the magnetic surfaces must be determined before the absolute particle flux

can be evaluated. The particle flux has a significant effect on the actual plasma confinement time and incorrect values for the particle flux will result in erroneous predicted confinement time.

To date, this approach has been successful only for neoclassical transport in the collisional (Pfirsch-Schlüter) and collisionless (banana) regime. Transport coefficients in the more difficult intermediate (plateau) regime have not been obtained, except for large aspect ratio, elliptic cross section tokamaks. Some progress has been made in understanding shape effects on MHD and kinetic drift instabilities, which may cause anomalous transport. The self-consistent methods correctly calculate transport coefficients for the time-varying geometry, properly include convection and adiabatic changes and within the limitations of the neoclassical models treated, can handle any aspect ratio, surface shape (including separatrices), and beta with equal case. In the collisional case only 1-D transport equations of standard from plus a 2-D equation equivalent to the equilibrium equation are required. In the collisionless case integrals are also calculated on each flux surface to describe trapped particles.

Even for the most sophisticated 1½-D models presently in use the required computer time is less than twice that needed for 1-D codes. For many simulation problems only minor changes in transport will result from adopting a 1½-D model and in these cases the additional complexity is probably not warranted. But for the class of problems described

above (and presumably for others) 1½-D models are already cost effective. Future problems such as transport from 3-D tearing or toroidal spin-up (due to momentum input from beam heating) may require a considerable increase in computer time.

B. Neoclassical Transport Coefficients

Although plasma exhibits a wide range of collective properties, most of this behavior takes place on a time scale shorter than the binary collision time. On a longer time scale, the so-called diffusion time scale, the plasma exhibits properties associated with collisional effects such as electrical conductivity, thermal conductivity, particle diffusion across or along magnetic field lines, etc. In order to calculate these macroscopic properties, transport coefficients must be obtained from the appropriate statistical description of the plasma. Transport coefficients are the quantities that linearly relate fluxes such as the energy flux, to forces such as the temperature gradient. When combined with the exact conservation laws for particles and energy and with Maxwell's equations, the linear transport relations provide a closed set of equations that predict the time evolution of the plasma, given a proper set of initial and boundary conditions.

The transport coefficients cannot be obtained by solving the so-called moment equations, since these are not a closed set of equations. For example, the first moment equation, called the momentum equation is obtained by taking an average over velocity space of particle velocities

weighted by the distribution function f(x,v,t). The equation for the first moment is of the form:

$$m \frac{\partial}{\partial t}(n \vec{v}) + \vec{\nabla} \cdot \tilde{P} - en\left(\vec{E} + \frac{1}{c} \vec{v} \times \vec{B}\right) = \vec{F}$$

where $\vec{v}$ is the mean velocity and $\tilde{P}$ is the stress tensor.

Solution of this moment equation would give the macroscopic velocity of electrons at a given point in the plasma. But this equation contains the stress tensor $\tilde{P}$ and the friction force $\vec{F}$. Closure relations for $\tilde{P}$ and $\tilde{F}$ in terms of the mean velocity are now available in all neoclassical regimes. However, viscosity and friction coefficients must be determined by solving for the distribution function. The fluxes can then be found by solving the fluid momentum balance equation given above. The distribution function for an ionized plasma obeys an integro-differential equation just like the Boltzmann equation for neutral particles except that it contains $e\vec{E}$ and $\vec{v} \times \vec{B}$ terms:

$$\frac{\partial f}{\partial t} + \vec{v} \cdot \vec{\nabla} f + \frac{e}{m}\left(\vec{E} + \frac{1}{c} \vec{v} \times \vec{B}\right) \cdot \frac{\partial f}{\partial \vec{v}} = C(f)$$

where C is the collision operator that conserves particles, momentum and energy. Whereas in the Boltzmann equation, the collision term represents binary collisions, in a plasma, collisions are not pre-

inary, because of the long range of the inverse square for Coulomb collisions.

The cumulative effect of small-angle collisions in a plasma is much more important than binary collisions. When a particle in a plasma is subject to simultaneous small-angle deflections, its progress in velocity space becomes a random walk superposed on the ordered motion due to macroscopic E and B fields. This yields an expression for the collision term of the Fokker-Planck type:

$$\left(\frac{\partial f}{\partial t}\right)_c = \frac{\partial}{\partial v_i}\left[-A_i f + \frac{1}{2}\frac{\partial}{\partial v_j}(B_{ij} f)\right] \equiv C(f)$$

where A_i and B_{ij} are "friction" and "diffusion" coefficients respectively. They are functions of x,v,t at which $\left(\frac{\partial f}{\partial t}\right)_c$ is to be calculated and are also linear functionals of f (x,t).

In transport theory applications, the Boltzmann equation is averaged over the rapid motion of a charged particle around a magnetic field line. The resulting equation, called the drift kinetic equation, has the form

$$\frac{\partial f}{\partial t} + (\vec{v}_{\parallel} + \vec{v}_d) \cdot \vec{\nabla} f + \frac{e}{m}\vec{E}_{\parallel} \cdot \frac{\partial f}{\partial \vec{v}_{\parallel}} = C(f)$$

where $\vec{v}_{\parallel}$ and $\vec{E}_{\parallel}$ are the components of particle velocity and electric field parallel to the magnetic field, and $\vec{v}_d$ is the drift velocity due to curvature of the magnetic field lines.

The equation used to calculate ion thermal conductivity is a drift-kinetic equation with the Fokker-Planck collision term that has been reduced to three independent variables: two velocity and one spatial

variable. One of the spatial variables is eliminated under the assumption of small poloidal gyroradius, the second spatial variable is ignorable because of toroidal symmetry. The third velocity variable is the angle of rotation around the magnetic field, which has been averaged out.

Since the MHD time scale is much shorter than the diffusion time scale, in the calculation of transport coefficients the geometry is considered fixed and the transport coefficients are calculated for a given geometry.

Present Status of Transport Coefficients

The neoclassical ion thermal conductivity κ_i has been calculated only in certain limiting cases. Expressions for general values of collisionality are known only in the large aspect ratio limit, while expressions for general aspect ratio and general geometry are presently available only in the collision-dominated and collisionless limits. In view of the importance of this transport coefficient in the interpretation of experiments on PLT and other large devices, κ_i for general geometry, aspect ratio, and collisionality should be calculated.

As was mentioned above, the drift-kinetic equation is in three independent variables: two velocity variables and one spatial variable (assuming axisymmetry and small poloidal gyroradius). It would be possible to solve this equation, and calculate the required moments, using a large computer such as the CRAY. It would obviously take too much time to solve the kinetic equation during the running of the transport code for all of the significantly different flux surface configurations and

collisionalities which occur. If all interesting geometries were specified by a small number of size and shape parameters, a table of values of κ_i could be prepared. With a minimum of three size and shape parameters, plus the collisionality, and assuming ten values of each parameter, it would still be necessary to solve the kinetic equation 10^4 times, and to make use of a table with this number of entries.

C. Microinstabilities and Anomalous Transport

One aspect of toroidal modeling that deserves attention is the influence of various microinstabilities on transport. The evidence from experiments points to the fact that the thermal transport of electrons is not governed by classical effects. Furthermore, there is difficulty in explaining the success of gas injection experiments on the basis of collisional transport. In addition, high frequency wave scattering experiments reveal the presence of density fluctuations indicative of drift wave disturbances. On the basis of these facts, one is led to believe that these anomalous processes are the result of microinstabilities.

The methods by which transport induced by microscopic fluctuation is modeled can be summarized as follows. It is assumed that the anomalous transport is the result of the appearance of some specific instability. A small amplitude non-linear or quasilinear analysis is performed to determine the relative size of the various transport coefficients. The magnitude of the fluctuations and the resulting transport are then related in some way to the degree of linear instability present. There

are areas of contention in each of the three steps just described. First, there is no universal agreement on which of the instabilities are important. Some of the modes thought to produce anomalous transport are the electron and ion drift modes, and drift-tearing modes. Secondly, the applicability of the methods by which one calculates the transport coefficients for a prescribed set of fluctuations has not been proved. For example, it has not been proved that electrostatic quasilinear theory is sufficient. If it is not, then the effect of fluctuations in the magnetic field is not known. Do the fluctuations lead to islands, stochastic wandering of field lines, or some other effects? And thirdly, in the absence of some demonstrated saturation mechanism, it is not known how the level of fluctuations can be related to the degree of instability. One approach favors a weak dependence on the linear growth rate in which case a precise determination of the growth rate is not needed. A second approach favors a rapid increase in fluctuation level as the profiles pass from a stable to unstable state, in which case, a precise determination of the growth rate is necessary.

Evaluation of the various methods and models is difficult owing to the fact that there are few experiments in which these anomalous transport processes can be isolated from other losses and that it is difficult in general to measure the relevant unknown quantities. However, transport codes can be useful in testing the various models and determining their effect on confinement. Progress in this field would be

aided by experiments on smaller devices under more rigidly controlled circumstances and by particle simulation of anomalous processes.

D. Treatment of Collisionless Ions in High Beta, Non-Circular Tokamaks

Fast ions are characterized by their large deviations from a flux surface and by their consequent non-local nature. Thus, to properly treat the slowing down and plasma heating resulting from Coulomb collisions, the full orbit topology must be used. There are two ways that may be used to do this — a Monte Carlo particle following code, or a treatment of the fast particles in their constants of motion space.

Monte Carlo codes are relatively straightforward but are very time-consuming since the basic time step is a small fraction of a bounce time. Monte Carlo fast ion codes exist at Fontenay-aux-Roses, Princeton, and other places. To effectively use these codes, the slowing-down process must be artificially shortened and so far, less than 1,000 particles have been used. If only moments of the fast ion distribution are required, this may give adequate statistics. But, there is some interest in measuring the fast-ion slowing-down distribution function and comparing it to theory. This requires the use of many more particles than have been used until now. A unique advantage of the Monte Carlo approach is the ability to handle ripples in the magnetic field. However, this requires even shorter time steps and consequently longer computer times. A disadvantage of the method is the lack of analytic results and hence it is very difficult to generate scaling laws or to predict trends.

The other approach to the problem is to express the Fokker-Planck equation in terms of the three constants of motion* which completely characterize the particle orbit in an axisymmetric tokamak. The bounce average of this equation describes how the constants of motion change due to collisions. This method is being explored at ORNL.

The advantages of the constants of motion method are its slow time scale (much longer than a bounce time) and its analytic nature. Thus, there is hope that good approximations can be made and that scaling laws can be derived. The disadvantage of the approach is the difficulty of bounce-averaging the Fokker-Planck equations, a process which must be redone each time a plasma profile or equilibrium changes.

Another approach is to use the "elements of the orbit" methods exploited in celestial mechanics. Here one computes a sample orbit using the constants of the motion. One computes the rate of change of the constants of motion and advances the orbit accordingly, thus avoiding the problem of bounce averaging the Fokker-Planck equation, or even solving the Fokker-Planck equation at all.

---

*One such set of constants of motion would be: speed of the particle, at a point, maximum value of flux function along the particle orbit and $\frac{v_{\parallel}}{v_{\perp}} = \rho$ at the same point.

APPENDIX I

The Baldur Code

Baldur is a 1-D tokamak transport code that has been written primarily for TFTR. The code features two hydorgenic species (D and T), two impurities, two species of neutral gas, neutral injection heating, α-particle heating, flexible transport models, and slow adiabatic compressions.

The code uses empirical rather than six-regime transport. It contains finite alpha slowing down plus loss cones for alpha particles. Particles from the beam are included in the density calculation. Effect of 1/3 and 2/3 energy component and the compression of the real velocity distribution function with injection represent an improved treatment of neutral beams.

The physics modules in the code can be divided into two groups pertaining to energy (Fig. 1) and particle (see Fig. 2) balance. They include electron and ion heat transport, ohmic heating, neutral beam heating, alpha-particle heating, slow adiabatic compression, impurity radiation, and neutral gas cooling. Modules dealing with particle balance include hydrogen and impurity transport (two hydroben and two impurity species), neutral gas transport (two hydrogen species), sources due to thermalized beam ions and sources due to thermalized alpha ions.

Numerical Features

The code uses predictor-corrector method and first-order extrapolation for the integration of nonlinear, parabolic, initial value partial differential equations. Monte Carlo techniques are used for neutral gas transport, neutral beam deposition, and alpha-particle orbits. Simple Fokker-Planck schemes are used to calculate neutral beam heating and alpha-particle heating.

Equations are finite-difference with variable spacing of the zones. Below is a brief description of individual physics modules contained in the code.

Transport Models. The following models can be included by input: neoclassical, pseudo-classical, Bohm, microinstabilities, empirical

$$K, D \sim n_e^x T^y \quad (x \sim -1, y \sim 0) \quad \sim (a/r)^x$$

Normally the empirical model is used, adjusted to fit PLT and Alcator confinement data.

$$X_e \sim 10^{17}/n_e \quad cm^2/sec$$

$$D \sim 10^{17}/n_e \quad cm^2/sec$$

$$K_i \sim \text{neoclassical}$$

An arbitrary mixture of the above-mentioned models can be specified. The code can also use the local drift mode and the trapped-electron mode to determine marginally stable profiles for different instabilities

for different collisionality regimes.

Fig. 3 gives a comparison between the experimental values of T_e as a function of $\bar{n}$ in Alcator and the values calculated with two different values of X_e. Fig. 4 gives a comparison between experimental and calculated energy confinement time as a function on $\bar{n}$ for Alcator.

Two Hydrogenic Species. Separate transport equations are solved for each species. Separate neutral gas treatment is provided for each species, with charge exchange between them. Thermalized beam ions are added to the plasma density.

Two Impurity Species. The module includes coronal equilibrium radiation for 47 possible impurities (H_e to U with Z = 92). Separate transport equations for each impurity are solved in the course of the calculation. The module contains an optional simple non-coronal equilibrium. Fig. 5 gives the power loss due to various impurities as a function of electron temperature.

Neutral Gas. A Monte Carlo algorithm calculates transport of two neutral gas species. Neutral gas sources consist of recycling of plasma off the wall, gas puffing (edge effect), charge exchanged neutrals from the beam (volume effect) and recombination (volume effect). The assumption is usually made that gas puffing and recycling produce 40 eV neutrals. Fig. 6 illustrates particle tracking geometry used in neutral transport module.

Neutral Injection. The energy deposition profile is calculated with the aid of a Monte Carlo algorithm. A simple multigroup Fokker-Planck scheme is used to calculate the slowing down and pitch-angle scattering of beam ions. Slow adiabatic compression of beam ions includes pitch-angle effects. Loss of beam ions due to charge exchange is included but the recapture is not. The module contains no orbit effects and no beam-beam collisions. Fig. 7 shows calculation of tangential injection in TFTR. Fig. 8 shows a calculation of the time rise of T_i and T_e with beam injection. The figures show the result of Fokker-Planck and multigroup calculations. Fig. 9 shows electron heating in PLT before and after injection as a function of radius.

Alpha-Particle Heating. A one-group Fokker-Planck scheme is used to calculate the energy deposition. Alpha-particles from beam-plasma and thermal reactions are included. Thermalized alphas are added to the plasma as an impurity. Loss cones are included for the first orbit. Loss cones and time-delayed heating are computed with Monte Carlo and Fokker-Planck schemes. Figs. 10 and 11 give the effect of I_p and the aspect ratio respectively on prompt alpha-particle losses. Fig. 12 gives density profiles for the creation of alpha-particles, the density of alpha-particles after losses have occurred, and the energy deposition by alpha-particles.

Slow Adiabatic Compression. The compression is done at the end of each time step. Beam ions are compressed but alpha-particles are not. The limiter can be expanded during compression to study the gas blanket.

TOKAMAK ENERGY FLOWS

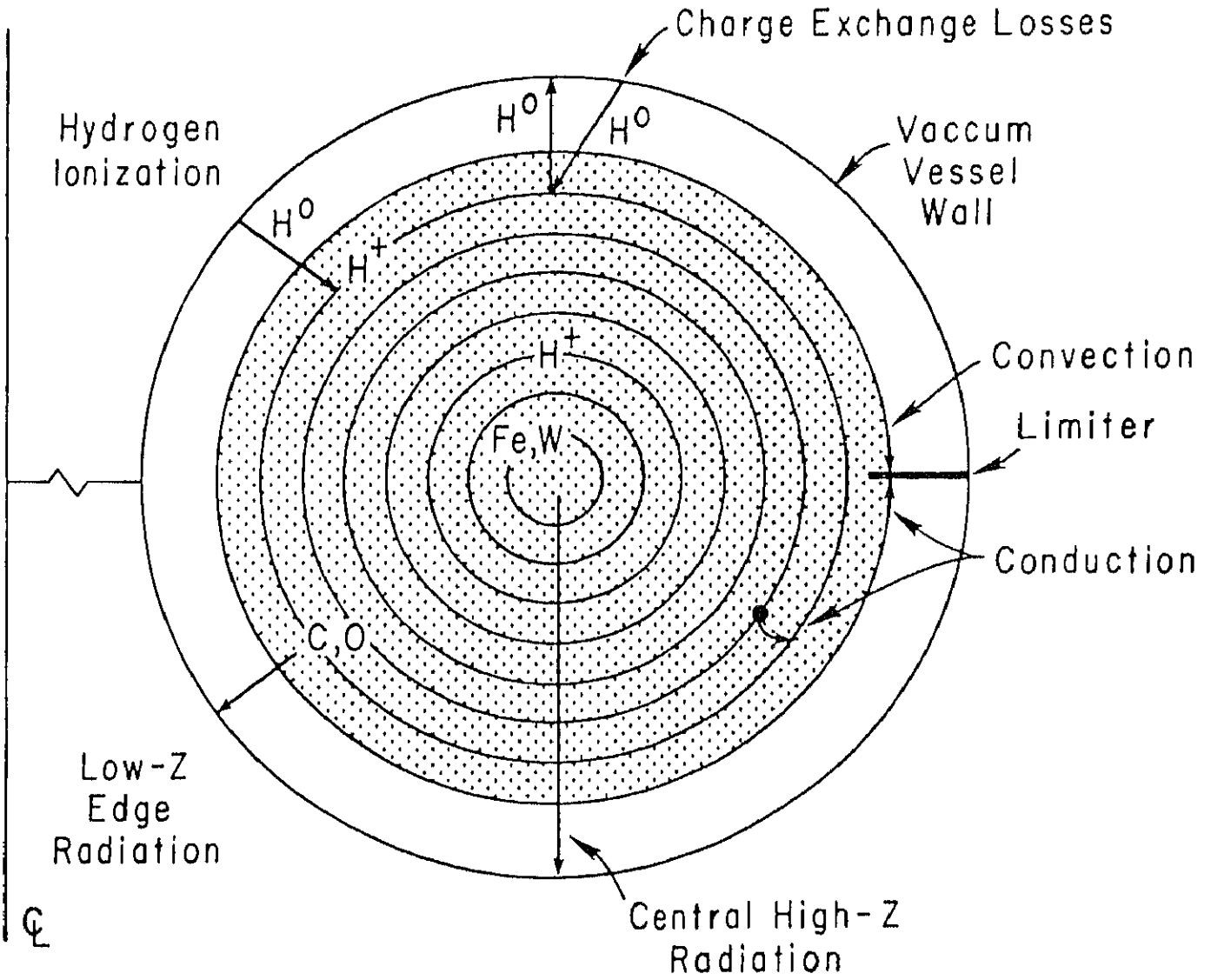

Fig. 1

PARTICLE BALANCE

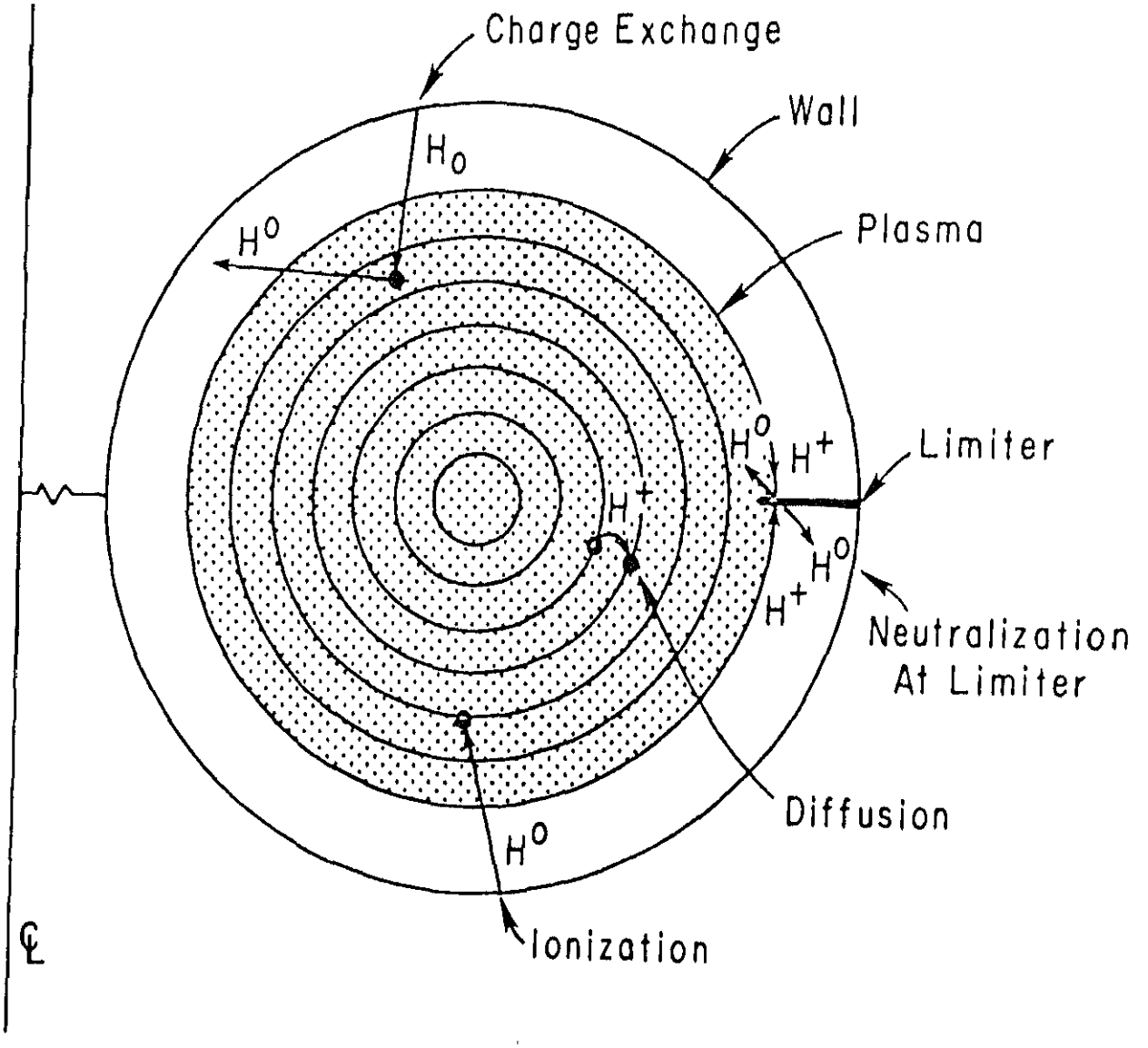

Fig. 2

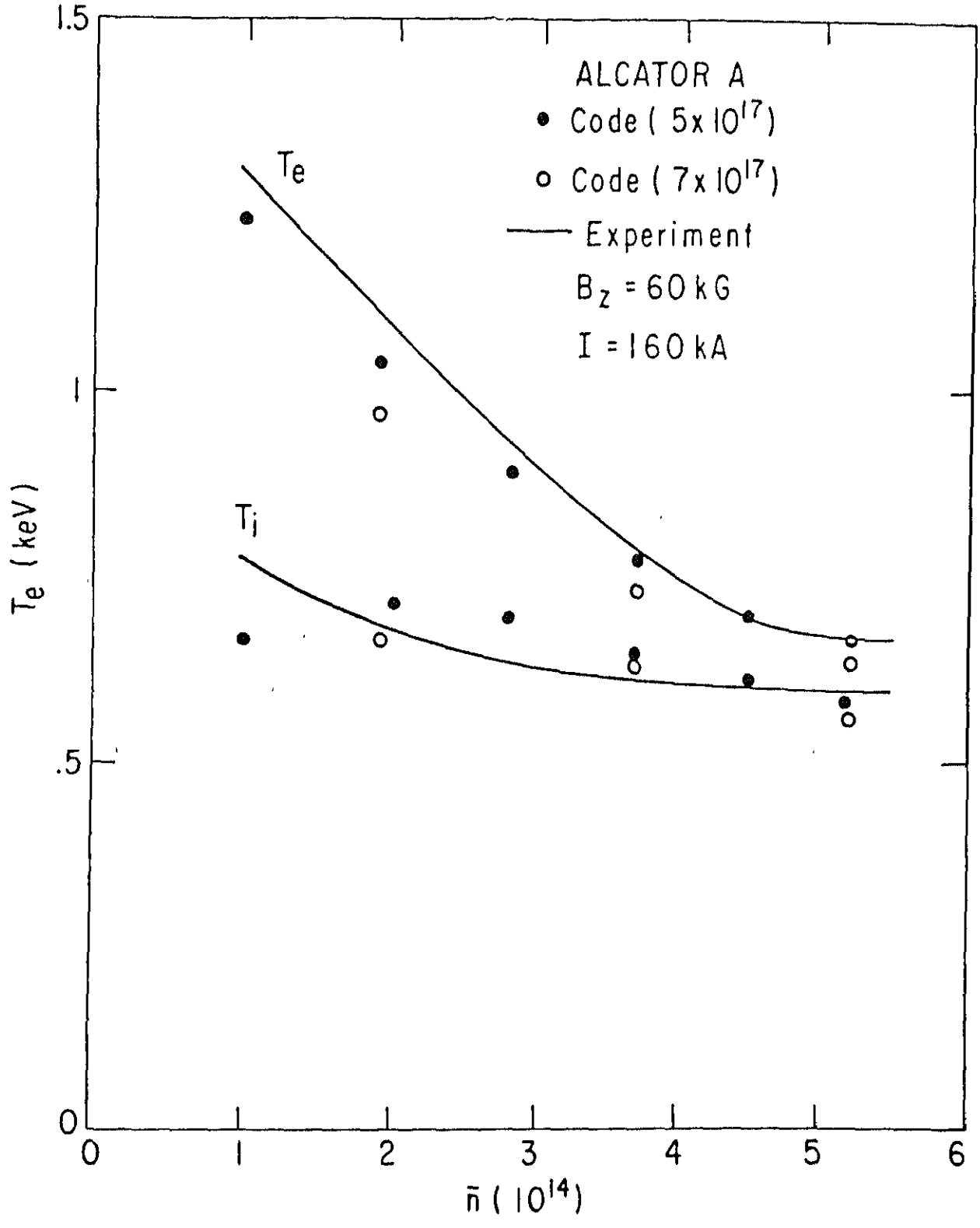
ALCATOR A
Code (5x10^17)
Code (7x10^17)
Experiment
B_z = 60 kG
I = 160 kA
T_e
T_i
T_e (keV)
n̄ (10^14)
1.5
1
.5
0
0
1
2
3
4
5
6

Fig. 3

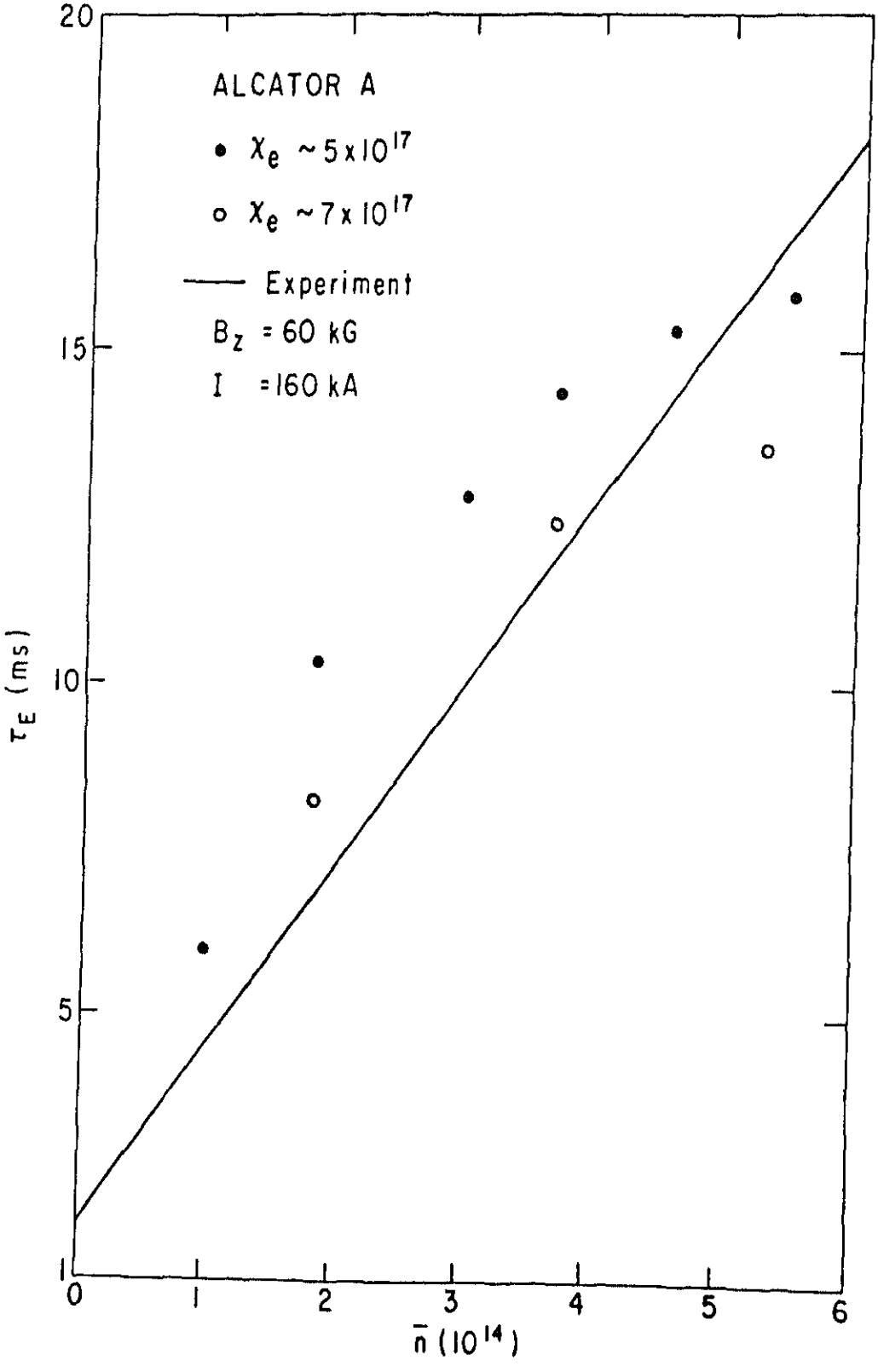
ALCATOR A
• $\chi_e \sim 5 \times 10^{17}$
o $\chi_e \sim 7 \times 10^{17}$
Experiment
B_z = 60 kG
I = 160 kA
τ_E (ms)
$\bar{n}$ (10^{14})
0
1
2
3
4
5
6
5
10
15
20

Fig. 4

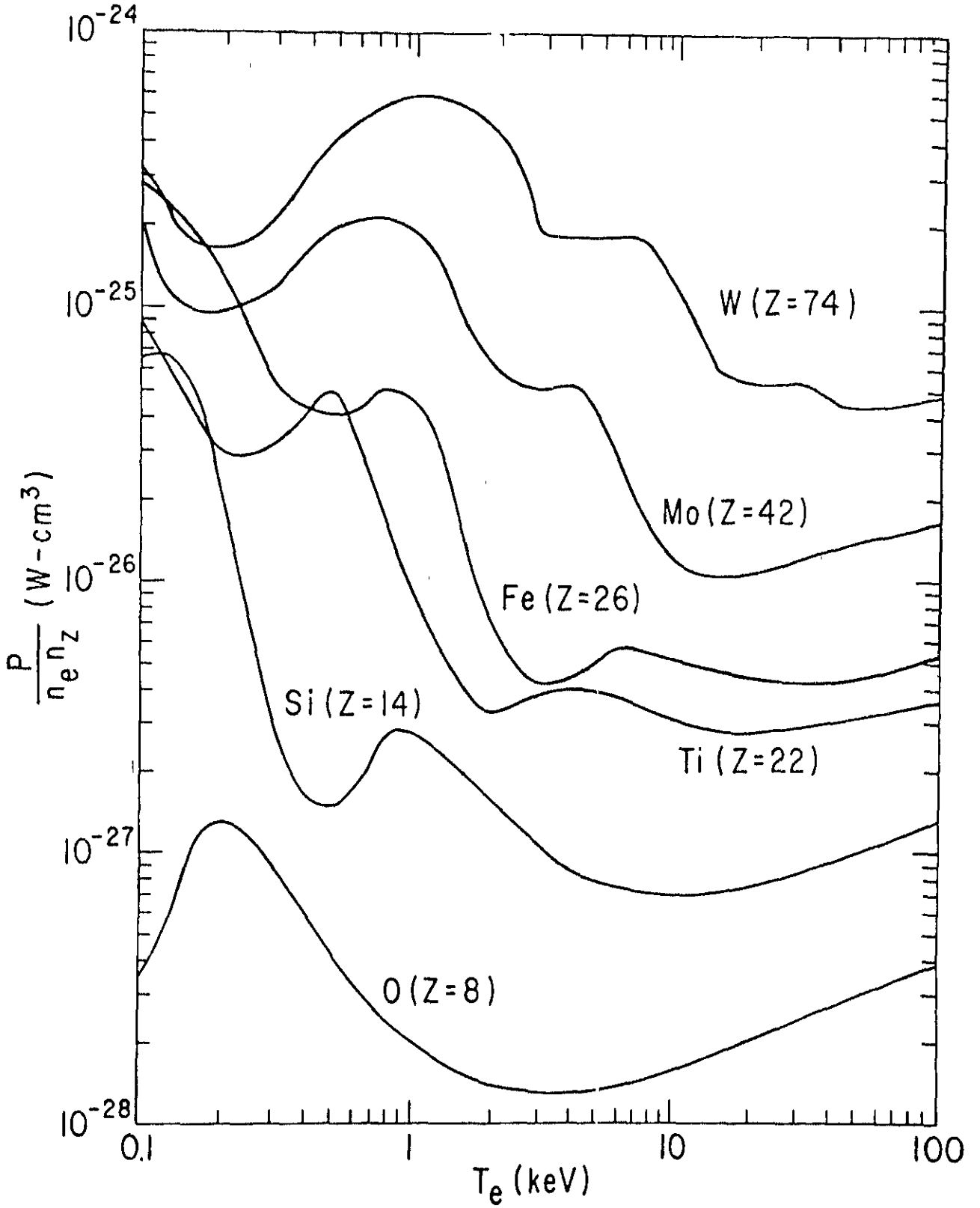
10^{-24}
10^{-25}
10^{-26}
10^{-27}
10^{-28}
$\frac{P}{n_e n_z}$ (W-cm^3)
W (Z=74)
Mo (Z=42)
Fe (Z=26)
Si (Z=14)
Ti (Z=22)
O (Z=8)
0.1
1
10
100
T_e (keV)

Fig. 5

GEOMETRY FOR PARTICLE TRACKING

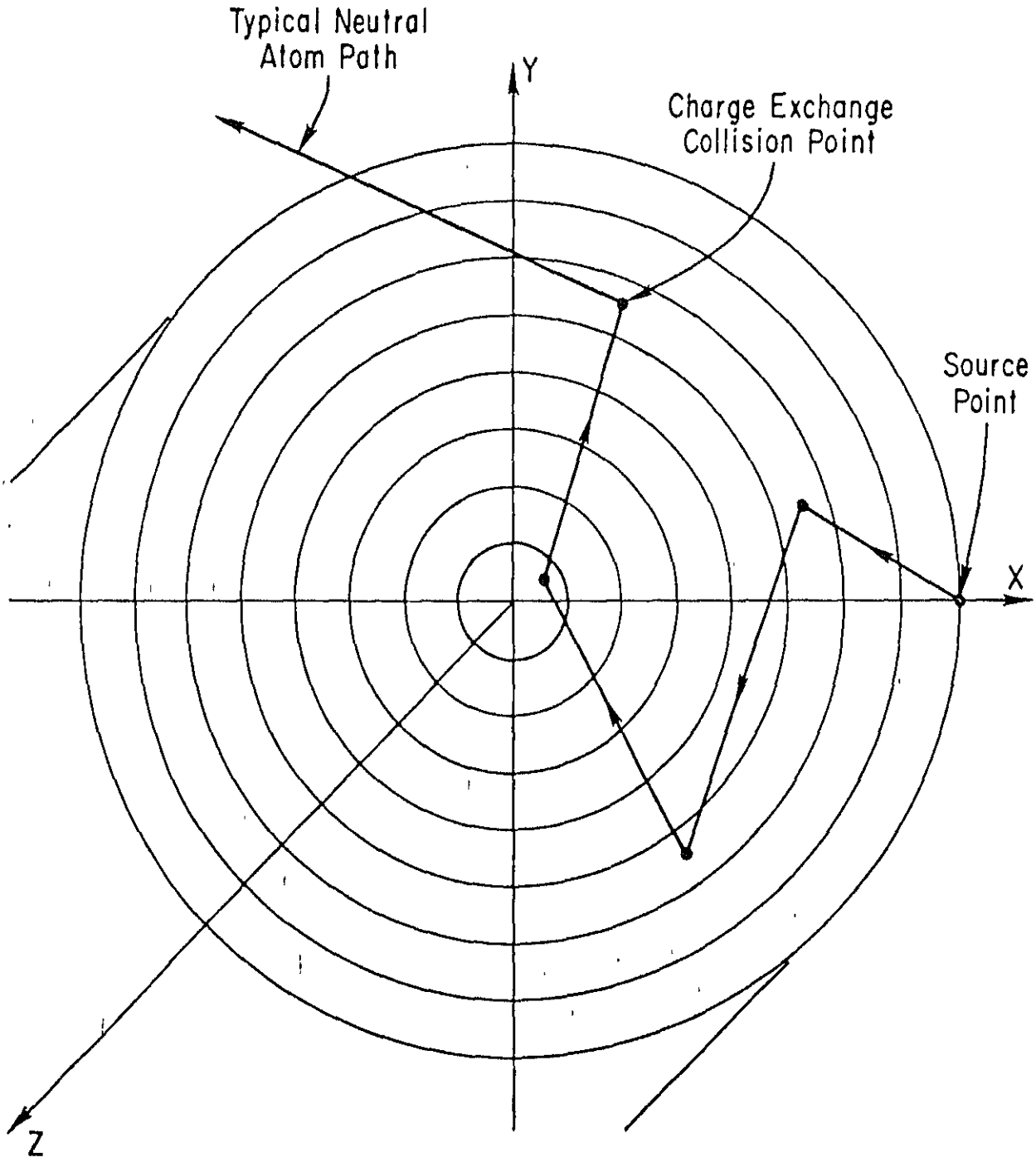

Fig. 6

TANGENTIAL INJECTION
TFTR STRONG COMPRESSION CASE

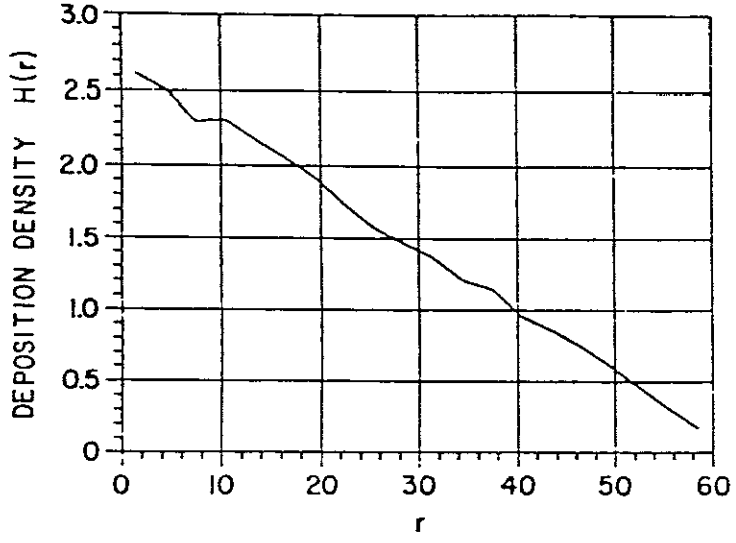

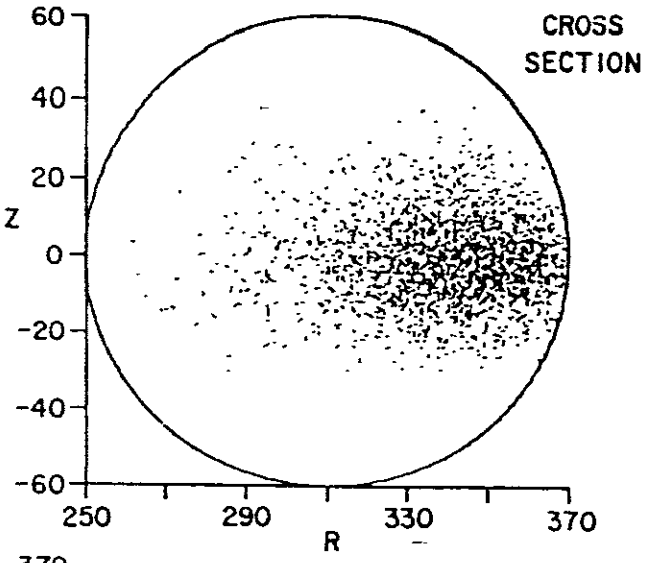

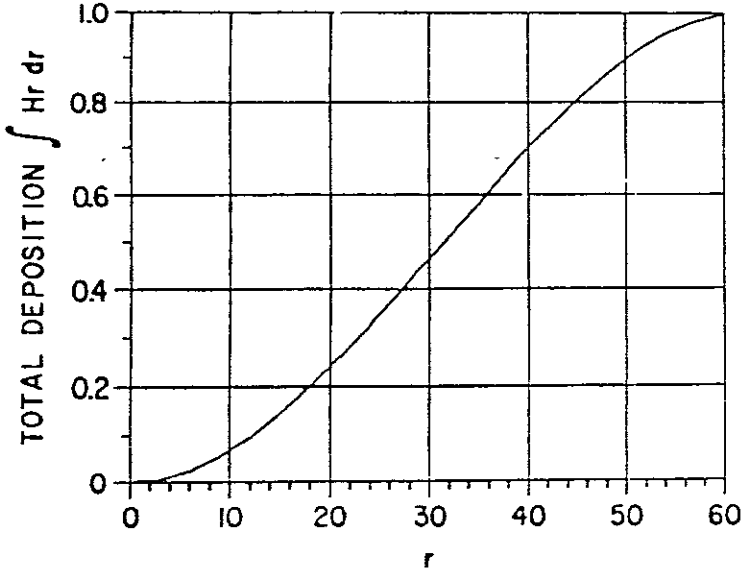

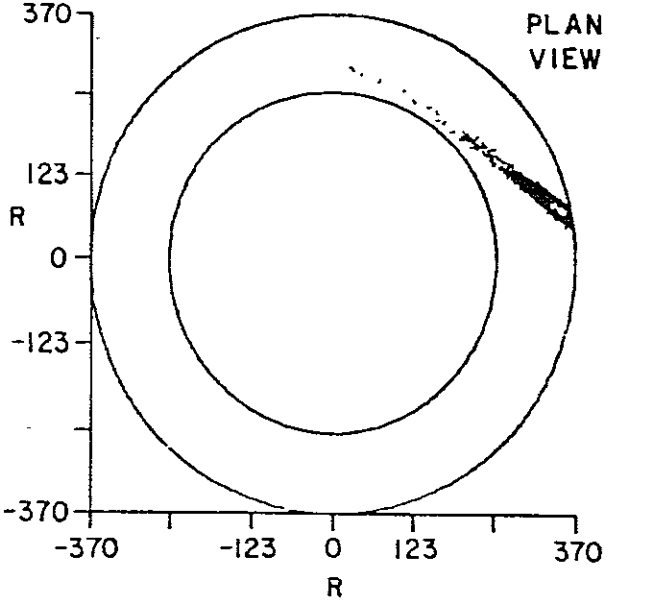

Fig. 7

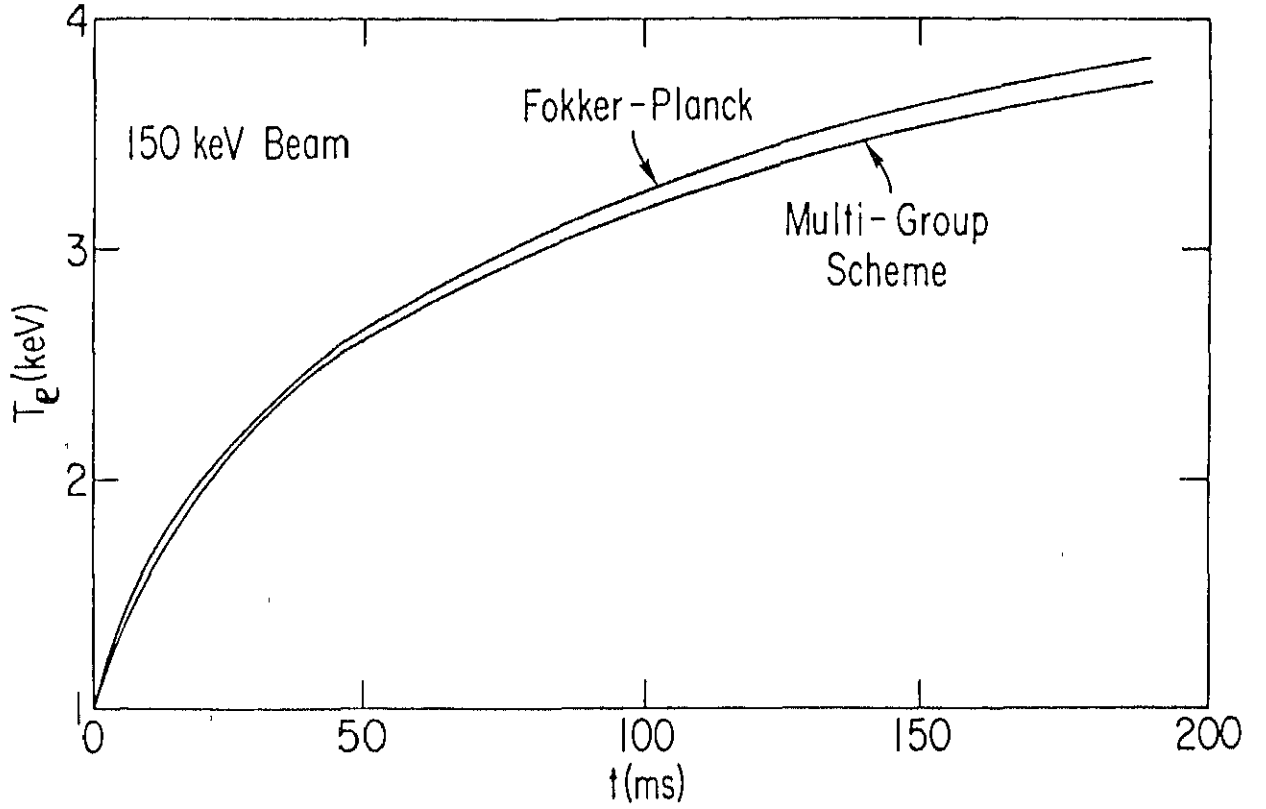
150 keV Beam
Fokker-Planck
Multi-Group
Scheme
T_e(keV)
t(ms)
0
50
100
150
200
1
2
3
4

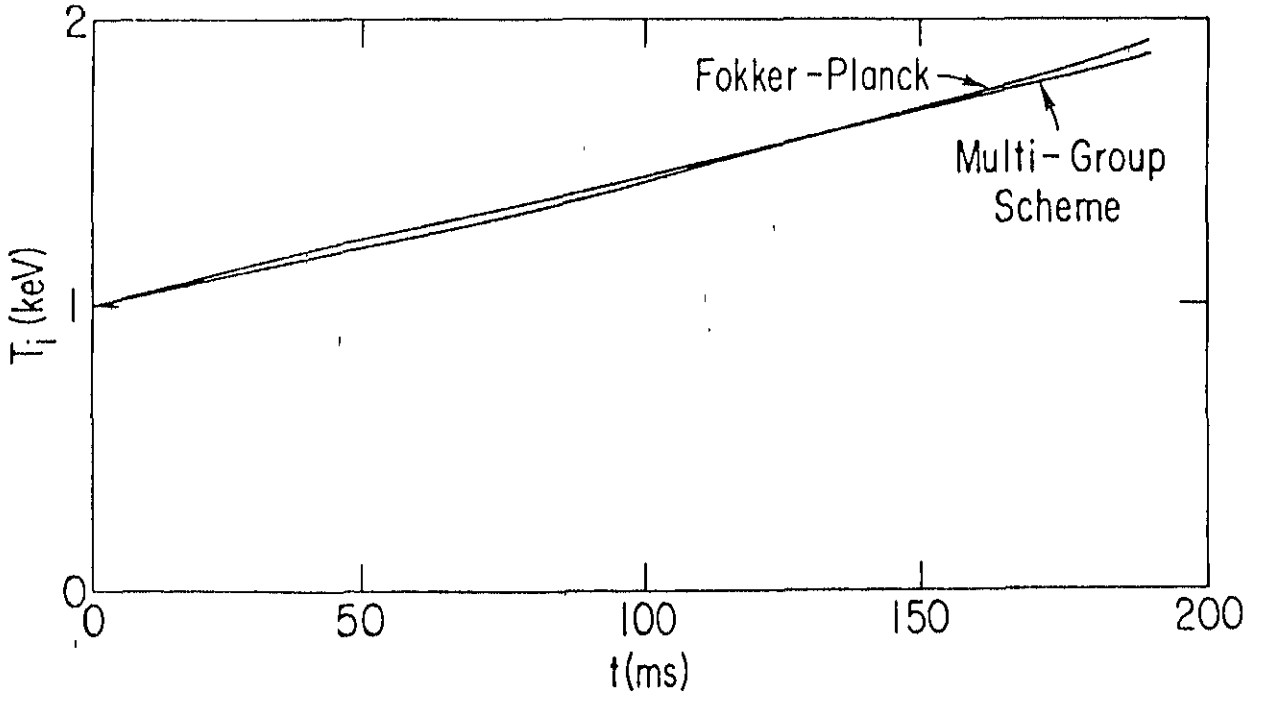
Fokker-Planck
Multi-Group
Scheme
T_i (keV)
t(ms)
0
50
100
150
200
1
2

Fig. 8

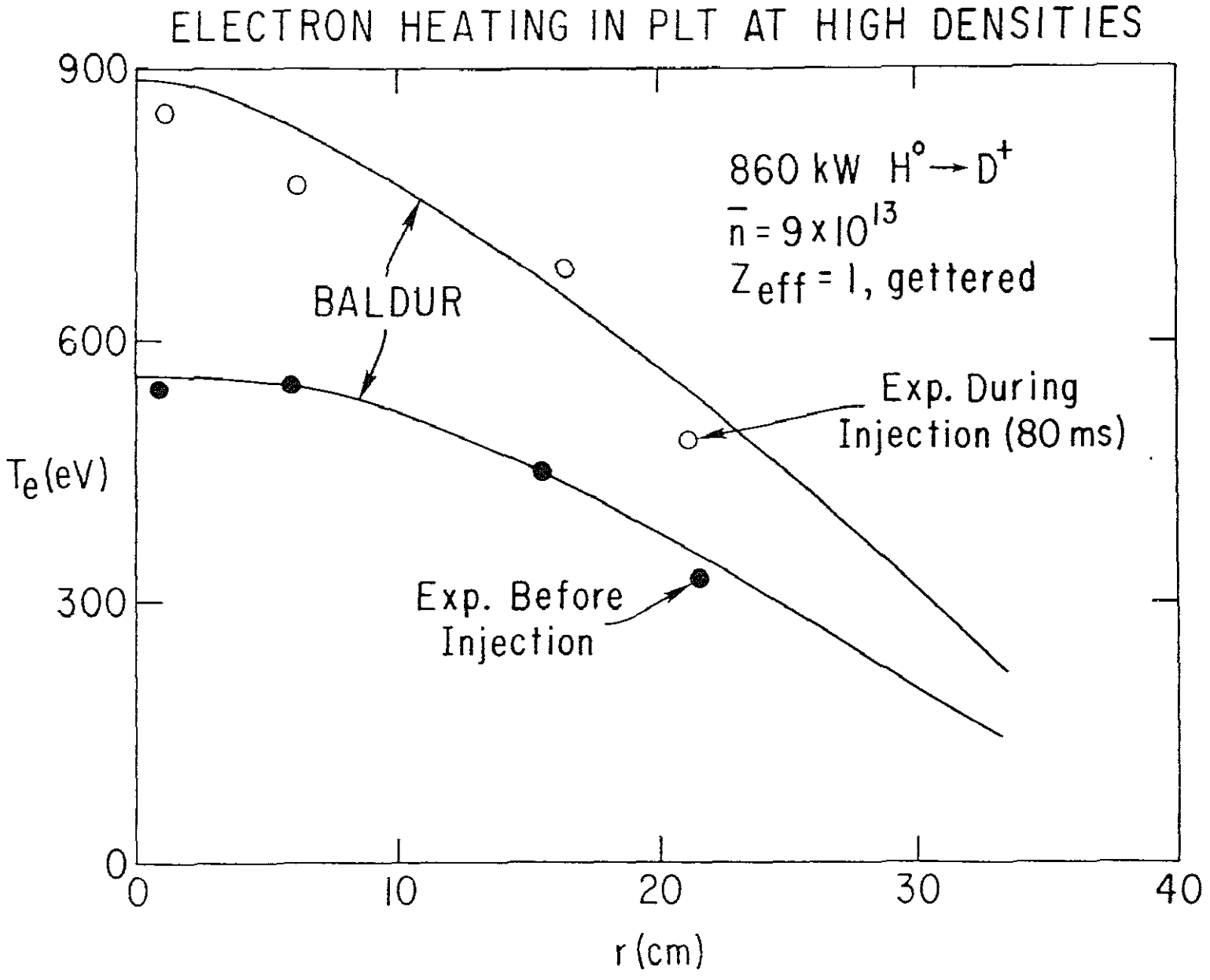
ELECTRON HEATING IN PLT AT HIGH DENSITIES
900
600
300
0
T_e(eV)
860 kW $H^0 \rightarrow D^+$
$\bar{n} = 9 \times 10^{13}$
$Z_{eff} = 1$, gettered
BALDUR
Exp. During Injection (80 ms)
Exp. Before Injection
0
10
20
30
40
r (cm)

Fig. 9

EFFECT OF I_p ON PROMPT ALPHA LOSSES

CURVE #	I_p(MA)	L_{TOT}
1	0.5	96%
2	0.7	72%
3	1.0	51%
4	1.8	21%
5	2.5	10%
6	4.0	3%
7	6.0	1%

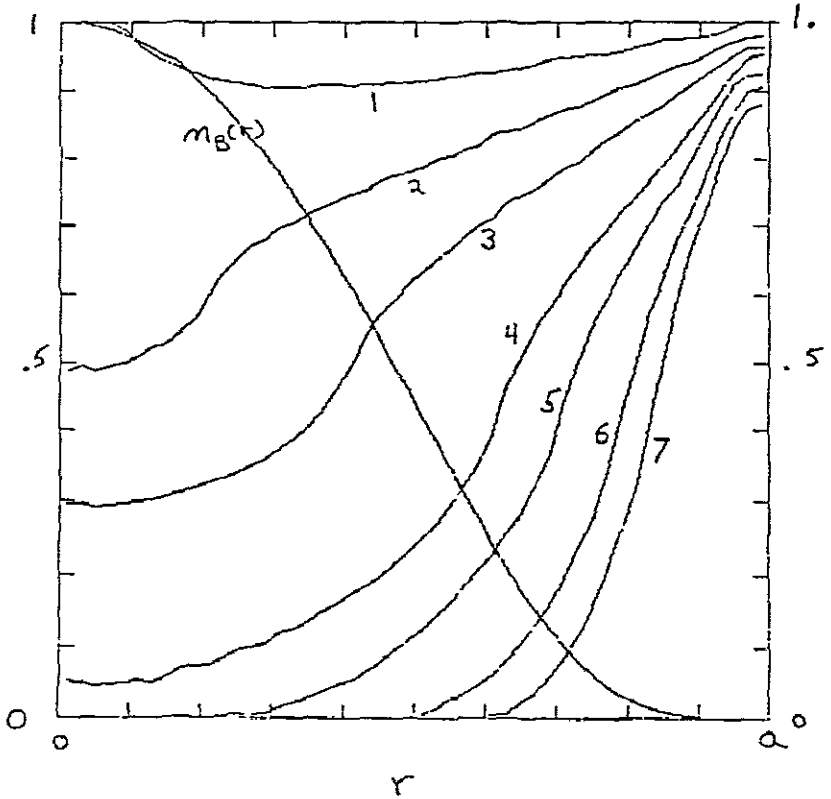

Aspect ratio R/a = 3

$m_B(r)$: ALPHA BIRTH DISTRIBUTION
INCLUDES PLASMA FUSION AND BEAM FUSION CONTRIBUTIONS

EFFECT OF ASPECT RATIO ON PROMPT ALPHA LOSSES

CURVE #	RMJ (cm)	L_{TOT}
1	170	22%
2	212	14%
3	255	10%
4	340	6%
5	510	2%

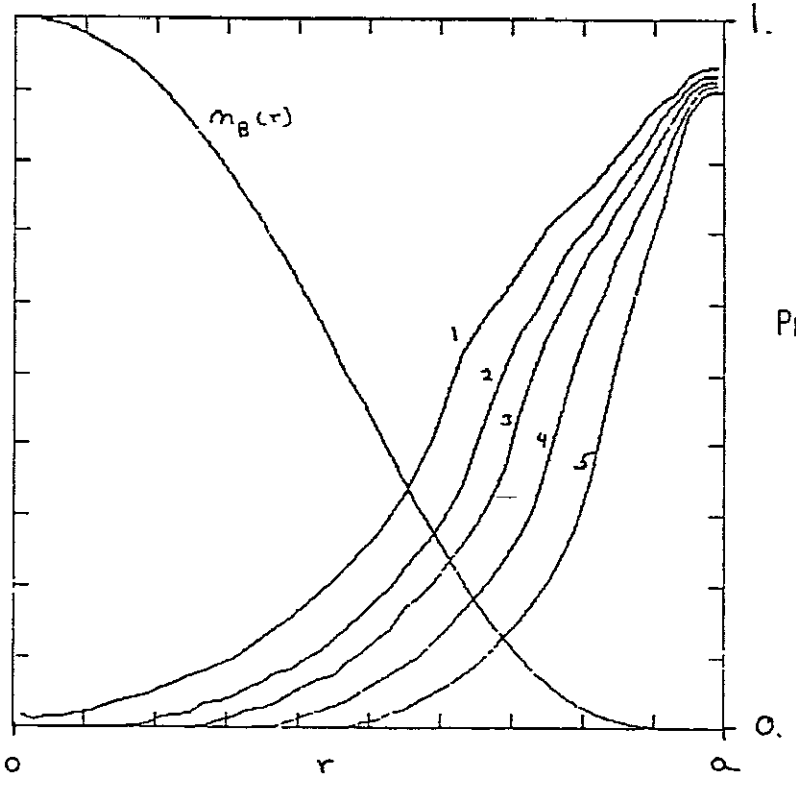

L (r)
PROMPT LOSS FRACTION

$m_\beta(r)$: ALPHA BIRTH DISTRIBUTION

DENSITY PROFILES FOR ALPHA BIRTHS, ALPHAS AFTER LOSSES, AND ALPHA ENERGY DEPOSITION

I_p = 2.5MA

L_{TOT} = 10%

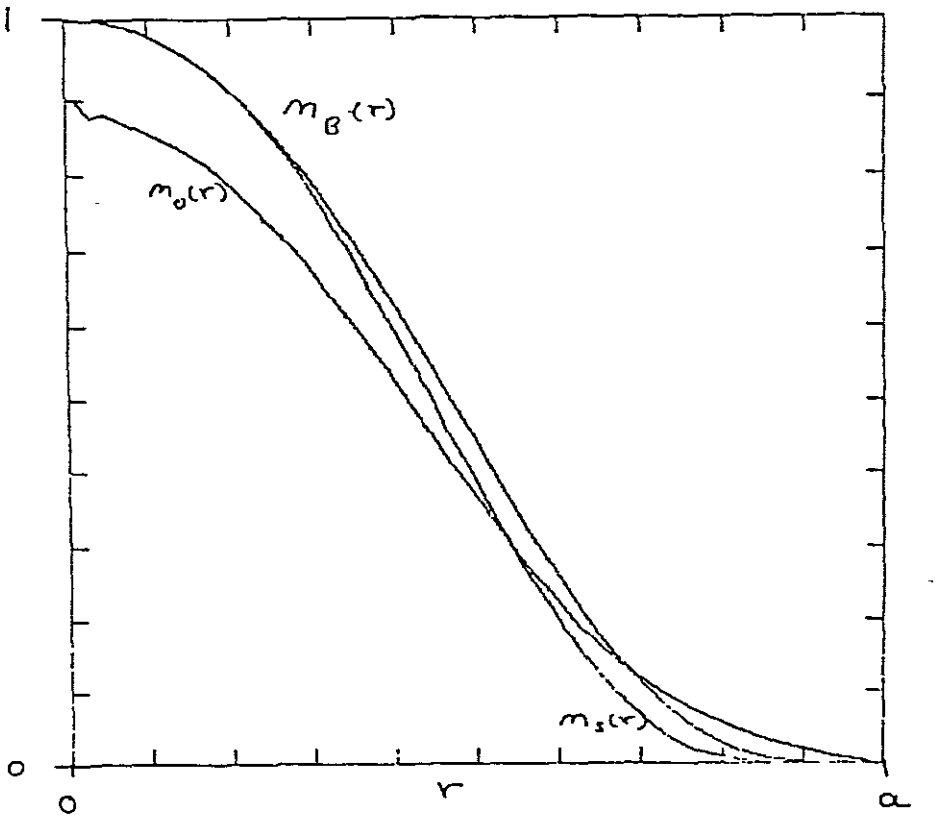

$m_B(r)$: ALPHA BIRTH DENSITY

$m_s(r)$: SURVIVOR DENSITY

$m_0(r)$: DEPOSITED ENERGY DENSITY

Fig. 12

APPENDIX II: NYU 1½-D TRANSPORT ALGORITHM

Introduction

The characteristic feature of the 1½-D family of algorithms is the separation of the solution process into alternate marching of profiles in 1-D (current, temperature, flux, volume, etc.) and 2-D evaluation of contours and geometrical coefficients (surface inductance, surface averaged resistivity, etc.). The basic present limitations of the 1½-D technique is to macroscopic, scalar pressure, MHD. Codes have been constructed and operated which include various combinations of finite β, general plasma cross section and aspect ratio, various topologies (Doublet, tearing, reversed-field mirror) including time-dependent transitions in topology due to external coil variation and plasma transport, with models including (classical) tensor resistivity and heat flow as well as the adiabatic limiting case.

The three most important advantages of these methods over fully classical (including inertia and wave motion) and the very recently developed 2-D marching of the Grad-Hogan model are:

1. Complex plasma geometry and topology, including dynamic changes in topology are easily managed;
2. The code logic is such as to be easily adaptable to convert any 1-D (cylindrical) "Kitchen Sink" transport code to a fully 2-D basis.

Extension of 1½-D techniques to closed line
completely 3-D toroidal transport seems now

DENSITY PROFILES FOR ALPHA BIRTHS, ALPHAS AFTER LOSSES, AND ALPHA ENERGY DEPOSITION

I_p = 2.5MA

L_{T_eT} = 10%

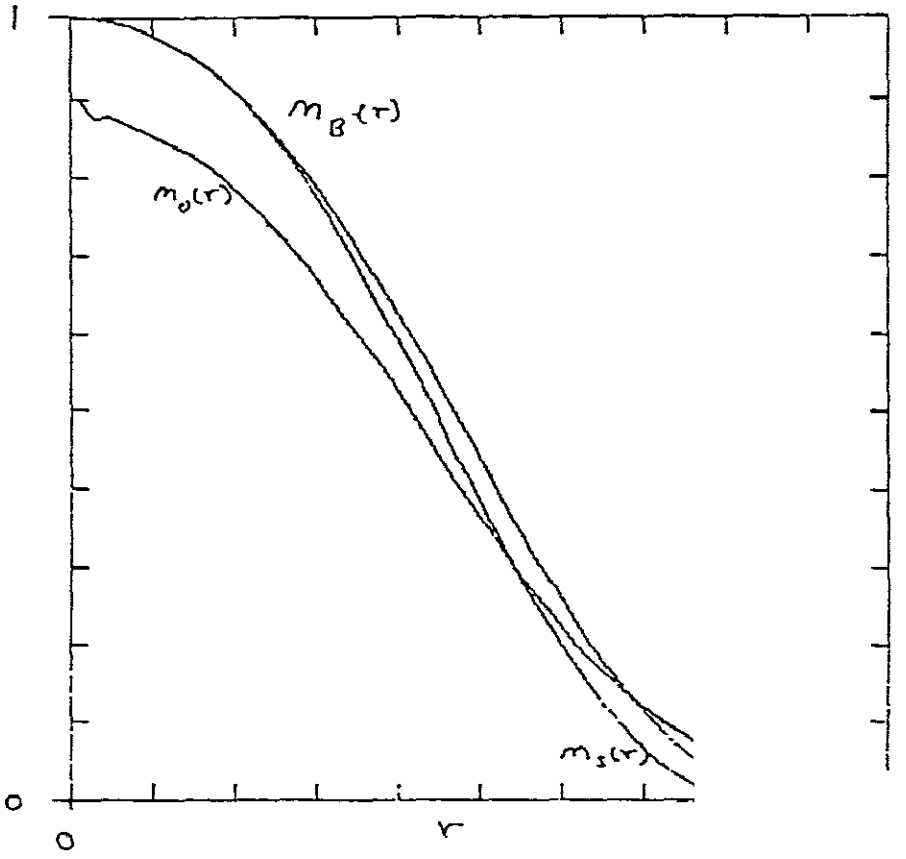

$m_B(r)$: ALPHA BIRTH DENSITY

$m_s(r)$: SURVIVOR DENSITY

$m_0(r)$: DEPOSITED ENERGY DENSI

Fig. 12

APPENDIX II: NYU 1½-D TRANSPORT ALGORITHM

Introduction

The characteristic feature of the 1½-D family of algorithms is the separation of the solution process into alternate marching of profiles in 1-D (current, temperature, flux, volume, etc.) and 2-D evaluation of contours and geometrical coefficients (surface inductance, surface averaged resistivity, etc.). The basic present limitations of the 1½-D technique is to macroscopic, scalar pressure, MHD. Codes have been constructed and operated which include various combinations of finite β, general plasma cross section and aspect ratio, various topologies (Doublet, tearing, reversed-field mirror) including time-dependent transitions in topology due to external coil variation and plasma transport, with models including (classical) tensor resistivity and heat flow as well as the adiabatic limiting case.

The three most important advantages of these methods over fully classical (including inertia and wave motion) and the very recently developed 2-D marching of the Grad-Hogan model are:

1. Complex plasma geometry and topology, including dynamic changes in topology are easily managed;
2. The code logic is such as to be easily adaptable to convert any 1-D (cylindrical) "Kitchen Sink" transport code to a fully 2-D basis.

Extension of 1½-D techniques to closed line 3-D (EBT geometry) and completely 3-D toroidal transport seems now possible. There is, however,

no consensus among the participants of the workshop on the degree of difficulty in accomplishing this task. Strongly anisotropic problems (such as guiding center or drift models for a mirror machine with loss cone) do not seem amenable at present. The neoclassical (guiding center or drift but approximately scalar pressure) problem seems to have reached a stage close to that of the classical MHD Grad-Hogan model some five years ago. The theory including consistent geometry changes seems to be visible but algorithms and operating codes for a 1½-D or 2-D version need further technological improvement.

The Basic 1½-D Algorithm

As mentioned before, one part of the code is an equilibrium solver. In 2-D, given $p(\psi)$ and $B_z = f(\psi)$ profiles, equilibrium is found by solving a nonlinear elliptic PDE,

$$\Delta\psi = F(\psi),\ F = -dp/d\psi - f df/d\psi \tag{1}$$

One method of solution is to iterate using a Poisson solver,

$$\Delta\psi_{n+1} = F[\psi_n(x,y)] = f_n(x,y) \tag{2}$$

This may or may not converge in cases where the solution is unique as well as when the solution is non-unique (i.e., after bifurcation). There is a large literature on more and more sophisticated procedures, but there is no universally dependable algorithm. In a case of multiple solutions, numerical stability (distinct from physical stability) determine which of the solutions may be found.

A second formulation of the equilibrium problem is

(3) $$\Delta\psi = F(V)$$

where the r.h.s. is a known function of V. The same iteration

(4) $$\Delta\psi_{n+1} = F(V_n),\ V_n = V_n(x,y) \sim \psi_n(x,y)$$

is usually more rapidly convergent than (1) but requires contours of ψ and volumes to be evaluated. The numerical stability of solution algorithms for (3) is different from (1) and both are different from physical stability.

A third equilibrium formulation, given adiabatic profiles $\mu(\psi)$ and $\nu(\psi)$ defined by

(5) $$p \approx \mu[\psi'(V)]^{\gamma}$$
$$f \approx \nu\psi'(V)$$

leads (for $\gamma = 2$ and $\nu = 0$) to the differential equation

(6) $$\Delta\psi = -\frac{d\mu}{d\psi}(\psi')^2 - 2\mu\psi'' \equiv R$$

The solution will amost never converge on simple iteration

(7) $$\Delta\psi_{n+1} = R_n$$

(and this gives no opportunity to impose proper boundary conditions). A method which converges extremely well is to alternate between the Poission equation

(8) $$\Delta\psi_{n+1} = R_n(x,y)$$

which is used to compute only the geometric contours ψ_{n+1} = const. (the ψ_{n+1} profile is discarded). Given the contours, the inductance

(9) $$K_n(V) = \langle |\nabla V|^2 \rangle$$

is calculated and the average pressure balance

(10) $$(K\psi')' = -\frac{d\mu}{d\psi}(\psi')^2 - 2\mu\psi''$$

is solved from an ODE for $\psi(V)$, given $\mu(\psi)$ [a priori] and given $K(V)$ [temporarily, by iteration]. From $\psi(V)$ and the previous contours, $V(x,y)$, one evaluates $R_{n+1}(x,y)$.

Incidentally, the ODE allows specification of ψ at the center ($V=0$) as well as the elliptic boundary condition at the plasma edge.

In a non-adiabatic problem with transport, the averaged (1-D) transport equations take the place of Eq. (10). In 2-D, a representative transport equation

$$\frac{\partial\psi}{\partial t} + u\cdot\nabla\psi = \eta\Delta\psi$$

when averaged becomes

$$\psi_t + U\psi' = \eta(K\psi')'$$

where

$$\frac{\partial \psi}{\partial t} = \frac{\partial}{\partial t}\,\psi(x,y,t), \quad \psi_t = \frac{\partial}{\partial t}\,\psi(V,t)$$

and

$$U = \langle u \cdot \nabla V \rangle = \oint u \cdot dS$$

If an adiabatic variable (e.g., mass) is taken as an independent variable

$$\psi_t + U\psi' = d\psi/dt = \frac{\partial}{\partial t}\,\psi(M,t)$$

the velocity U (the plasma diffusion velocity) is eliminated and the entire set of transport equations becomes a set of 1-D transport equations in M and t, with various geometrical coefficients similar to K.

There is always one fewer averaged transport equation than originally (since one of the "diffusing" variables is taken as the independent 1-D variable). The count is made up by adding the average pressure balance (10) [in an appropriate independent variable, not necessarily V].

The skeleton algorithm is:

1. From initial equilibrium calculate (contour averaged) coefficients for 1-D averaged transport equations. These are marched in 1-D, together with the average pressure balance for many diffusion time steps for one geometry time step.

2. Using the diffused 1-D profiles at the advanced geometry time step, a r.h.s. R(x,y) is computed for the Poisson equation. [Here one has a choice, involving simplicity, accuracy, stability, etc. of using the forms (1) or (3) or (6) since all profiles are available from the result of diffusion].

There are two iteration loops, the inner one to solve for a geometry $F(\psi)$ or $F(V)$ or $\mu(\psi)$, and the outer one which repeats the diffusion over a geometry time step until all geometrical profiles such as $K(V)$ converge.

One can take $K(V,t)$ to be piecewise constant in t, or make it linear in t between geometry steps (for insertion in the transport equations), or more sophisticated (e.g., predictor-corrector).

There are at least three (and preferably four) independent meshes

1. 2-D - (x,y)
2. 1-D - contours in (x,y) to evaluate averages
3. 1-D - diffusion
4. 1-D - interpolation among other meshes.

Also two semi-independent convergence criteria ε_i and ε_0 uter loops. The optimization problem is formidable oal. For example, in studying the small resistivity c, there is a very sharp moving singularity in $K(V,t)$

at the separatrix; this requires careful non-uniform contour placement. To optimize computer time, more sophisticated extrapolations of K(V,t) in t must be used, varying the values of ε_i and ε_0, the relative sizes of 2-D contour, and diffusion meshes, must be performed to reduce the running time. In one problem at NYU dealing with transition from a Belt Pinch to a fully formed Doublet with practical parameters, proper use of contours and diffusion meshes made it possible to run the code with only five updates of the geometry.

In a transition from circular to D-shaped (or change induced by increasing beta) it should rarely be necessary to use more than two or three geometry calculations; but this will have to be confirmed in different parameter ranges.

More details of the equations and algorithms are found in the following publications:

1. Grad, H., Hu, P. N. and Stevens, D. C. "Adiabatic Evolution of Plasma Equilibrium," Proc. Nat. Acad. Sci., USA, 72, pp. 3789-3793 (1975).

2. Grad, H., Hu, P. N., Stevens, D. C. and Turkel, E., "Diffusive Transition from Belt Pinch to Doublet," 2nd European Conf. on Computational Physics, Computing in Plasma Physics and Astrophysics," Garching, Germany, April 27-30, 1976.

3. Grad, H., Hu, P. N., Stevens, D. C. and Turkel, E. "Classical Plasma Diffusion," IAEA 6th Conf. on Plasma Physics and CTR, Berchtesgaden, Germany, Oct. 6-13, 1976.

4. Grad, H., Hu, P. N. "Classical Diffusion: Theory and Simulation Codes," Workshop of High β Plasma, Varenna, Italy, Sept. 1977. Also Rept. MF-91, DIMS, NYU, March 1978.

5. Oak Ridge National Laboratory, Theory Department Memo #75/9.

A proof of existence (not convergence of the numerical algorithm) has been given for a linearization of the GDE [G. Vigfussen, Thesis, NYU, 1977] which is the basis of the 2-D marching algorithm employed by Jardine (PPPL) for the Grad-Hogan model (these linearized versions are even more useful for analytical work than numerical).

APPENDIX III: A 2-D RESISTIVE TOKAMAK AND DOUBLET TRANSPORT CODE

I. Purpose:

1. To construct an efficient "1 1/2 D" transport code in the Grad-Hogan formulation.

2. To investigate the range of validity of Pfirsch-Schluter diffusion.

3. To investigate the coupling between geometry and skin effect, geometry and plasma diffusion, skin effect and plasma diffusion.

4. To construct an efficient MHD code with real geometry as a foundation for next generation "Kitchen Sink" Tokamak and Doublet simulation.

5. To compare resistive with adiabatic transition from Doublet to Belt Pinch.

6. To investigate current profile evolution resulting from geometry changes.

7. To investigate plasma compression on the skin time scale.

II Description

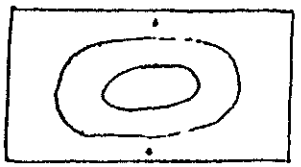

1. Low β, scalar pressure, classical resistivity, MHD.

2. 2D, plasma separated from rectangular box by vacuum region with coils.

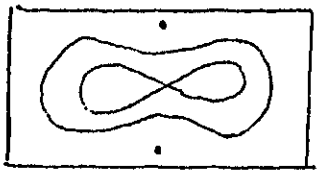

3. Toroidal and poloidal external field individually varied.

4. Primarily on resistive skin time scale (slower plasma diffusion superposed).

5. Tokamak, Belt Pinch, Doublet, and time dependent transitions.

6. Ability to handle low resistivity (adiabatic transition) with accompanying large, localized current layers (at plasma edge and at separatrix).

7. Plasma edge BC with skin effect and skinless.

8. Specialized to $\gamma = 2$.

III. Equations

Low β formulation [Nice, 1970]

$$\frac{\partial \psi}{\partial t} + u\cdot\nabla\psi = \eta\Delta\psi - c(t)$$

$$\Delta\psi = J(\psi,t) \qquad \left[J = -\frac{dP}{d\psi},\quad P = p + \frac{1}{2} f^2\right]$$

$$\langle u\cdot\nabla\psi\rangle = U_o\psi'$$

$$U_o = a(t)V\ , \qquad a = -\frac{1}{f_o}\frac{df_o}{dt}$$

U_o is the plasma compression induced by changing zero-order toroidal vacuum field, $f_o(t)$.

The net plasma <u>diffusion</u>, $U_1 = \oint u\cdot ds$ $(= \langle u\cdot\nabla V\rangle)$ is higher order on the skin time scale and can be commuted (separately) by the formulas

$$U_1 = U_p - K\psi'\psi_t - V\int_V^{\bar{V}} (J\psi')_t\, dV - \int_o^V V(J\psi')_t dV \qquad \text{[Grad-Hogan]}$$

or

$$U_p = -\eta Kp' - cK\psi' \qquad \text{[Pfirsch-Schluter]}$$

The complete formulation as used for computation is

$$\psi_t + U_o\psi' = \eta(K\psi')' - c$$

$$\Delta\psi = F\ , \qquad F = (K\psi')'$$

IV. Boundary Conditions

1) A poloidal boundary condition $\psi = \bar{\psi}(t)$ [usually constant in space, but not necessarily] is applied on the external rectangular box.

2) Coils (in this code, symmetrically placed) carry varying currents $I_c(t)$ which also influence the poloidal field.

3) The toroidal vacuum field $f_o(t)$ can be varied thru the convection term U_o. If f_o is constant, the plasma volume V_p is constant [otherwise $V_p f_o$ = const.].

4) In this scaling, poloidal field pressure is not strong enough to compress the plasma; changing $\bar{\psi}$ (or I_c) will, however, induce a skin current unless a special skinless BC (taken from the adiabatic problem) is used. In most cases, one of the following BC's has been used

   a) $\bar{\psi}$ = given at box

   b) $K\psi'$ = const. at $V = V_p$

   c) ψ' = const. at $V = V_p$

BC (b) (constant total plasma current) gives a skin current layer; BC (c) can be shown to coordinate (higher order distinct from f_o) toroidal and poloidal knobs so that there is no skin boundary layer.

5) At V = 0 a conventional heat equation natural BC is imposed on ψ.

6) Treatment of Separatrix is described separately.

V. Basic Algorithm

For a given $K(V,t)$, ψ is marched by solving a conventional 1D diffusion equation in $0 < V < V_p$ with conventional BC at $V = 0$ and choice (usually of (b) - skin or (c) - skinless) at V_p.

In an early version of this code [results presented at Madison, 1976], the separatrix was ignored and the two symmetric islands were treated as described in Code 1, taking $V = V_1 + V_2 = 2V_1$, as independent 1D variable and assuming that ψ and $K\psi'$ are continuous across the Sep. (essentially by ignoring its location or existence). A later, more accurate version is described in Sec. VI.

$K(V,t_i)$ is calculated in 2D at intervals t_i by taking $J(V,t_i) \rightarrow J(x,y,t_i)$ from the diffusion equation, inverting $\Delta\psi_\ell = J(x,y)$ and computing a new $K(V,t_i)$ from the contours of ψ_ℓ. Between t_i and t_{i+1}, K is assumed to be linear in t. The <u>outer loop</u>, assuming that all quantities are known at t_i, diffuses to t_{i+1}, recomputes K_{i+1}, diffuses again from t_i to t_{i+1} with the new K until convergence.

The <u>inner loop</u> is an iteration at a given time t_i, given $J(V)$, in which ψ_ℓ and the contours are iterated, $\Delta\psi = J[V(x,y)]$,

$$V(x,y) \rightarrow \psi(x,y) \quad \text{[Poisson]}$$

$$\psi(x,y) \rightarrow V(x,y) \quad \text{[volume within contour]}$$

VI. Separatrix Singularity and Normalized Variables

At the separatrix, K is unbounded as log $|V-V_s|$; this is nontrivial since $K' \sim 1/|V-V_s|$ occurs in the inhomogeneous term, $J = (K\psi')'$, of the Poisson equation. The actual singularity can be evaluated analytically and is not quite so bad. For a moving singularity, $K \sim \log$, in a diffusion equation $\psi_t = \eta(K\psi')'$ the current density is bounded but has a cusp almost at the separatrix (preceded by a smooth dip, if η is sufficiently small). The height of the cusp is unbounded as η becomes small.

The following normalized independent variables are taken, inside and outside V_{sep}

$$\hat{V} = V/V_s \qquad 0 < \hat{V} < 1$$

$$\hat{V} = (V-V_s)/(V_p-V_s)\ , \qquad 0 < \hat{V} < 1$$

In $(\hat{V}, t)$ the diffusion equation has a convection term, $(\dot{V}_s/V_s)\psi'$. Both $V_s(t)$ and $K(\hat{V}, t)$ are obtained from the geometry at intervals t_i, K by linear interpolation in t, and $V_s(t)$ by a cubic spline (so that $\dot{V}_s(t)$ is continuous at t_i).

A moving log is fitted to K near $V = V_s(t)$ by taking a pair of contours close to V_s on each side. $K = a_i + b_i \log |V-V_s|$ is

to each side (i = in, out); b_i is replaced by $\frac{1}{2}(b_1 + b_2)$

to the last contour on each side. The log fit

ch difference with a very fine 2-D mesh, but it

s accuracy with a coarse mesh (which cannot see

VII. Meshes and Interpolation

A fine mesh is used separately on each side of the Sep. for 1D diffusion. K, evaluated on contours (a fixed number outside, varying with V_s inside), is transferred to the diffusion mesh by cubic interpolation. The fine diffusion mesh is also used for transfer of J(V) to the 2D mesh by linear interpolation. The contour spacing has several alternatives:

1) number of contours and distance of first contour from Sep. give a geometric spacing (constant ratio of adjacent spaces),
2) number of uniformly spaced contours specified,
3) optional subdivision of "last" sibdivision (near V = 0 and near $V = V_p$).

Although possibly unreasonable at first glance, the combination of 1D and 2D meshes allows very fine resolution with moderate 2D mesh and contours (say 32×64 and 10 outside contours) in which a very sharp current profile of total width less than one 2-D mesh is accurately resolved, and an accurate cusp is drawn.

A number of algorithms for further improving the accuracy of description of small islands has not yet been fully implemented.

The equilibrium solver is very sensitive where the current peak at the Sep. is very large (a small change in $\dot{V}_s$ makes large changes in $J(x,y)$]. The outer loop is found to have properties similar to an asymptotic series when the current peak is large (small η and small island); viz. there is an optimum outer loop time step $t_{i+1} - t_i$; if too large or too small, many iterations are required.

In a transition from simple geometry to islated, the code first notices a change in topology in the 2D Poisson inversion. If the island is too small, it is ignored (no contours are close) and $K(0) = 0$ is used together with all finite, simple contours.

When the island is large enough to fit three internal contours (plus $V = 0$ and the Sep.) after convergence of the geometry at t_i, K is computed on <u>two</u> normalized meshes and transferred to the diffusion mesh before diffusing to t_{i+1}. At the same time, ψ is recomputed over the island region using $(K\psi')' = J$ and the new K.

VIII. Auxiliary Algorithms

1) The outer loop is almost always oscillatory (this can be qualitatively justified theoretically). There is therefore a great advantage in convergence to back-average the bare result of iteration with the previous iterate. A simple exercise in control theory adjusts the back average coefficient in terms of the observed convergence rate.

2) Back averaging is used in both outer and inner loops; the former on the 1D array, J(V), and the latter on the 2D array, ψ_ℓ.

Not yet implemented.

a) Refining 2D mesh in Box which surrounds island.

b) Using analytic formulas for K(V) in small island, extrapolating back to precise time of islation with analytic growth $\sim t^{3/2}$.

IX. Results

1. Sample results including a demonstration of enormous deviations from Pfirsch-Schluter were reported at the Sherwood Theory Meeting, 1975, and published in the Second European Conference on Computational Physics, Garching, 1976.

2. Very accurate current response to deformation, including a current spike precursor before islation, transient skin effect signature at the <u>center</u> of the plasma from oscillatory external coils, calculation of ηJ^2 heating at plasma center from oscillating separatrix current, and accurate reversible (half sine wave) operation at small η were reported at Berchtesgaden in 1976.

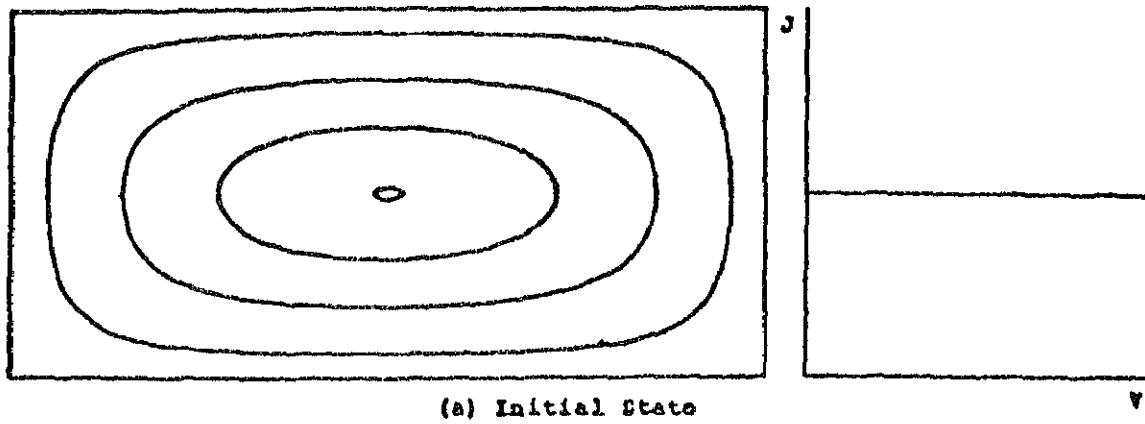

(a) Initial State

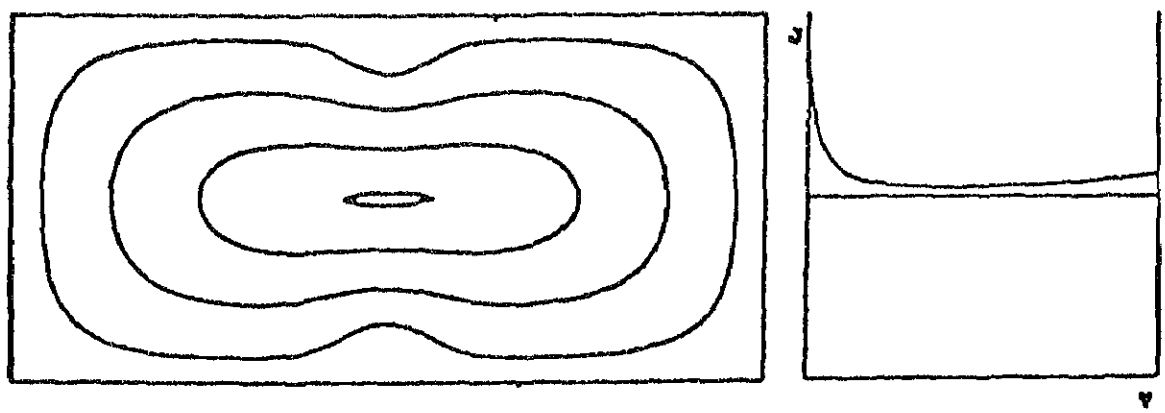

(b) Before Isletica

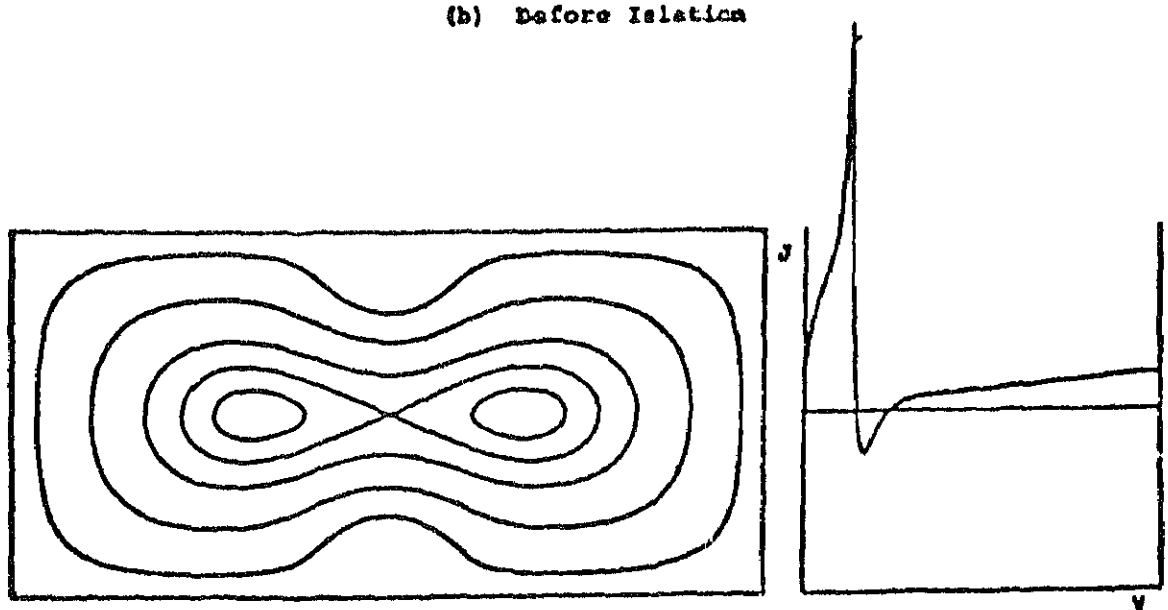

(c) Fully Developed Islands

Transition from Belt Pinch to Doublet.

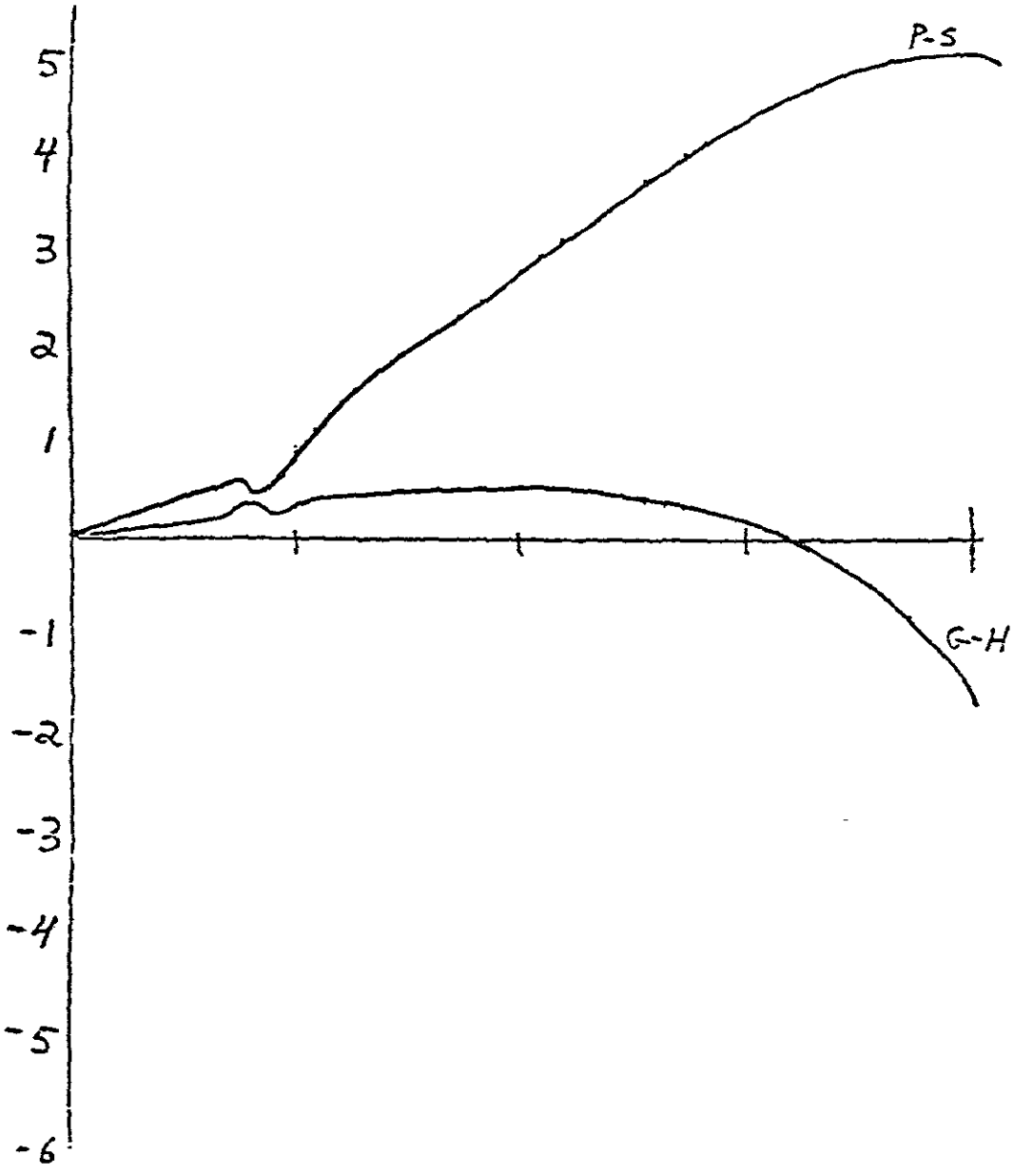

Coil = 1.7

GA SERIES

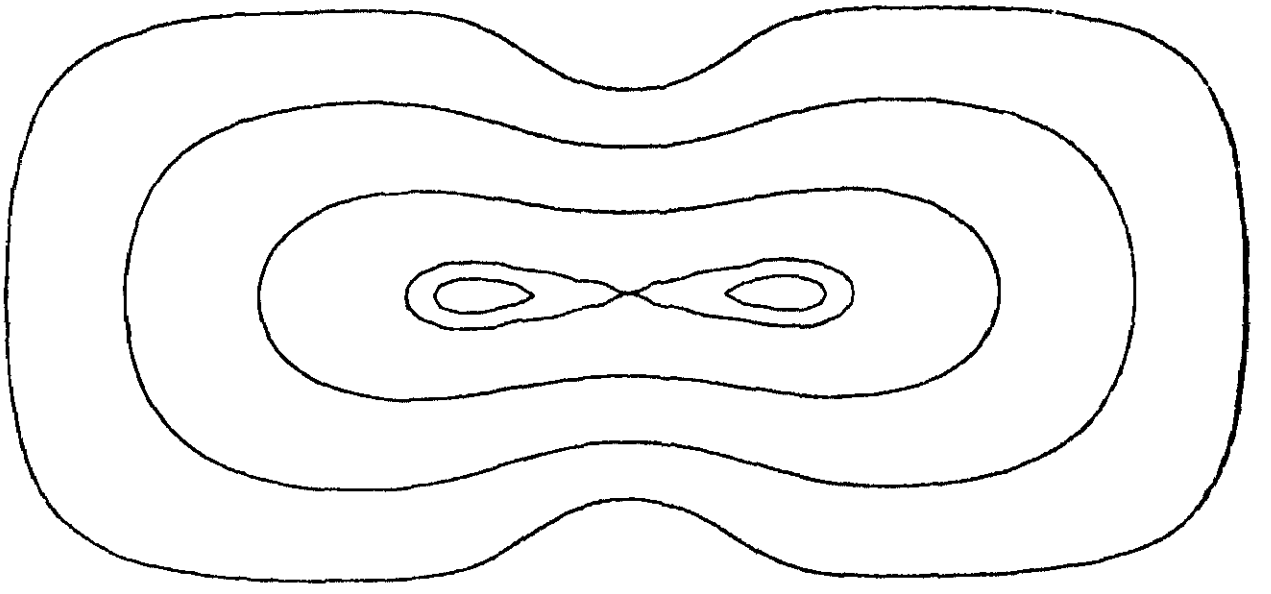

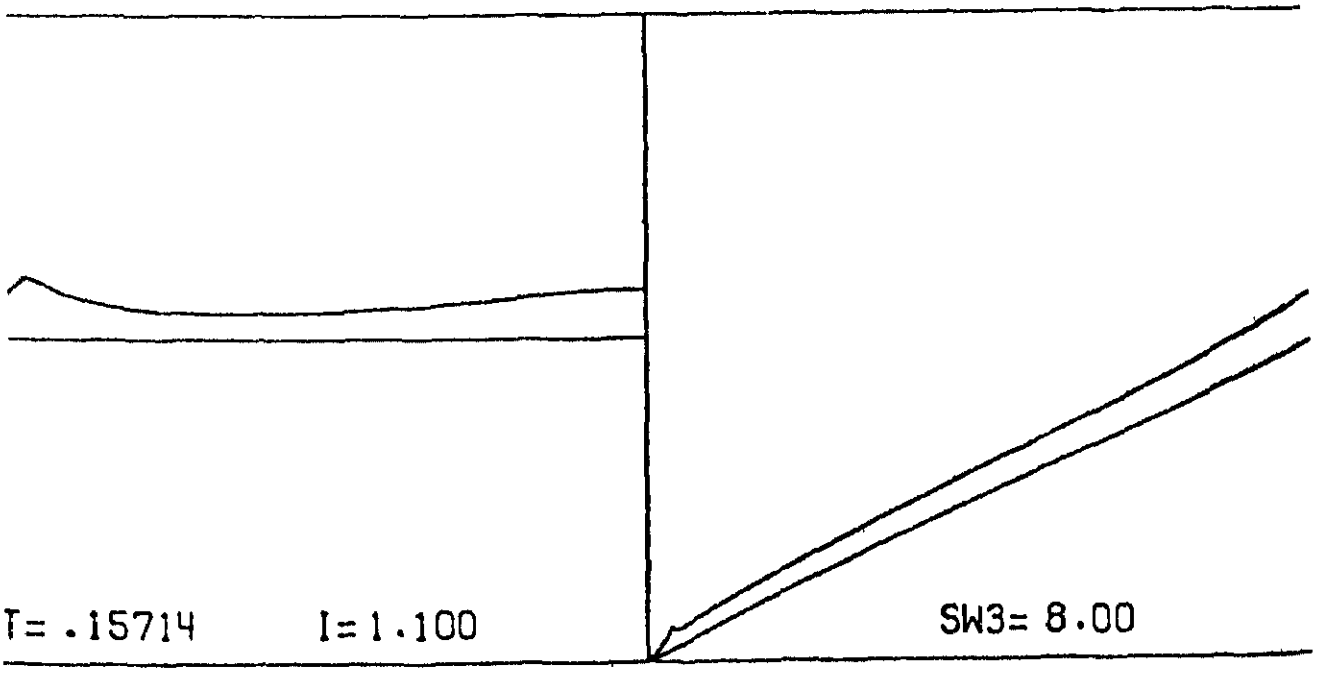

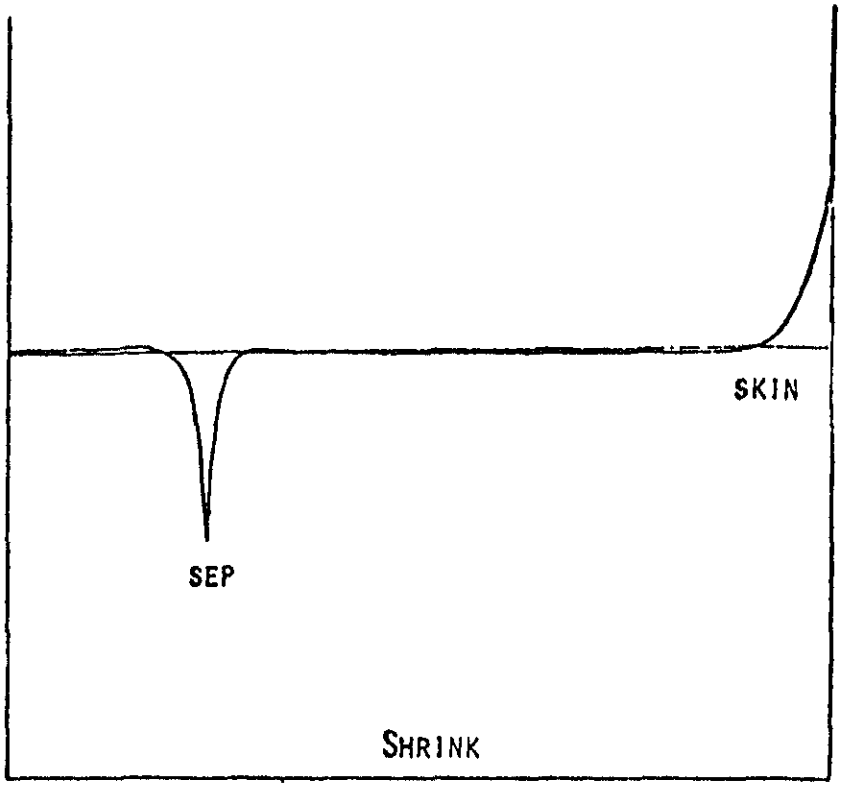
SKIN
SEP
SHRINK

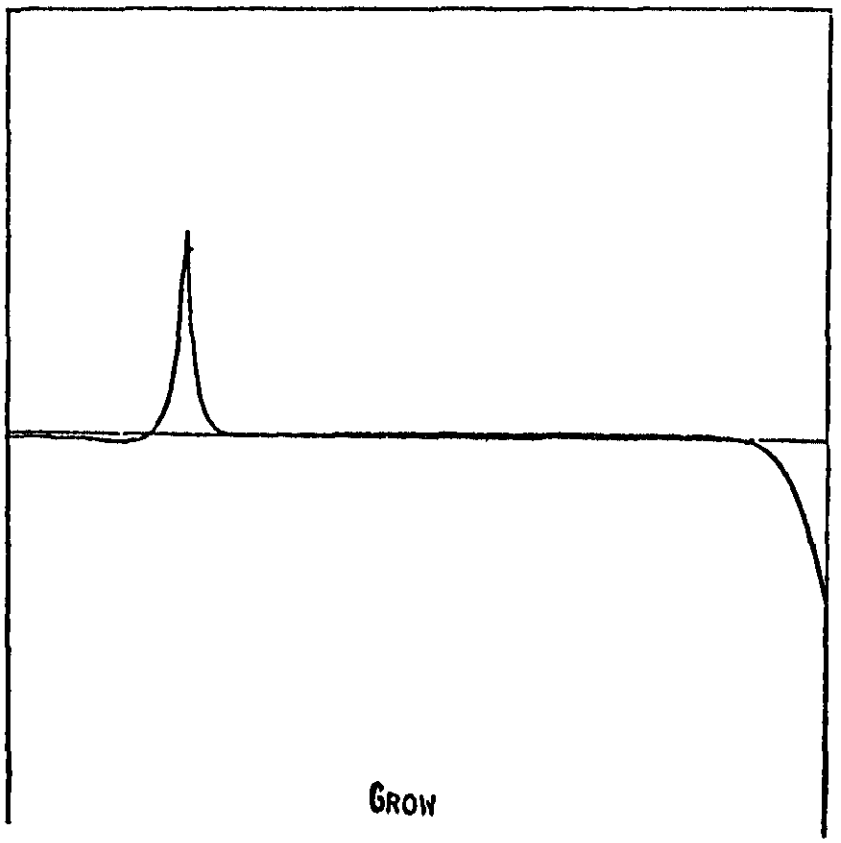
GROW

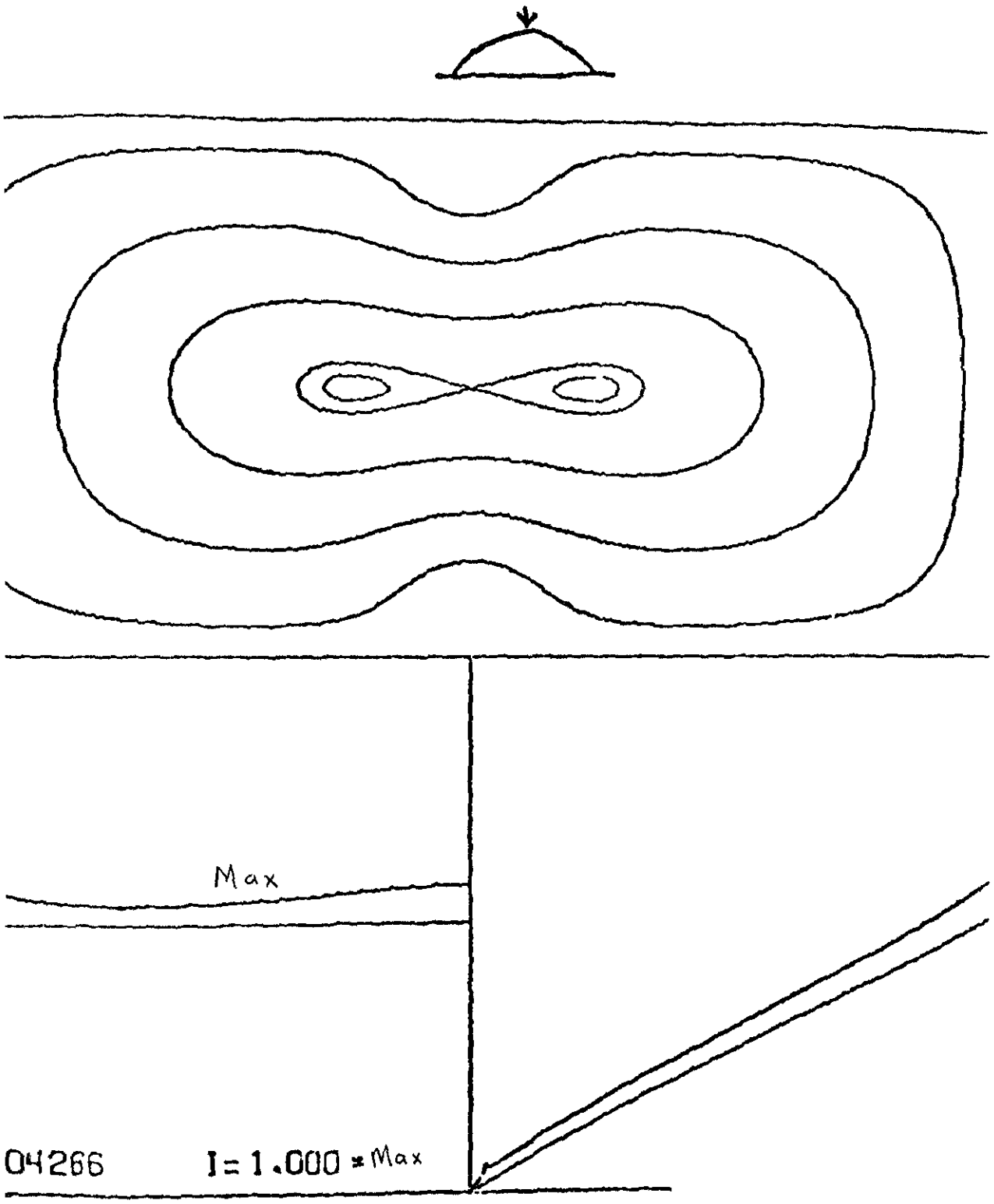
Max
04266
I = 1.000 * Max

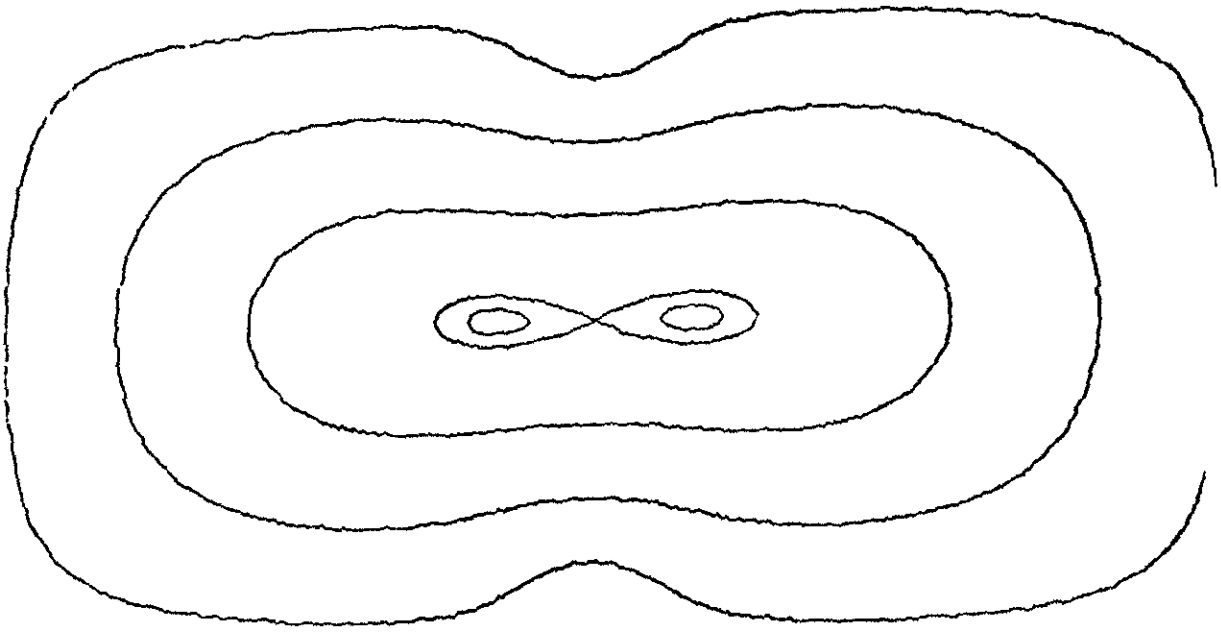

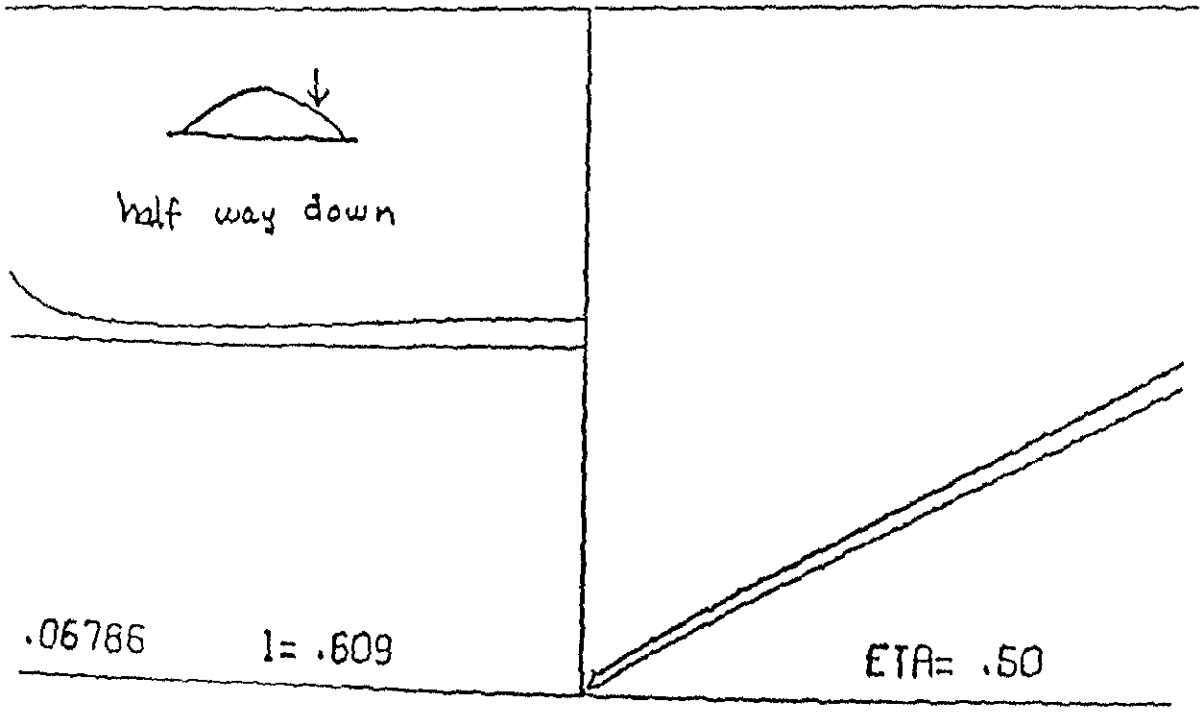
Half way down
.06786
l= .609
ETA= .50

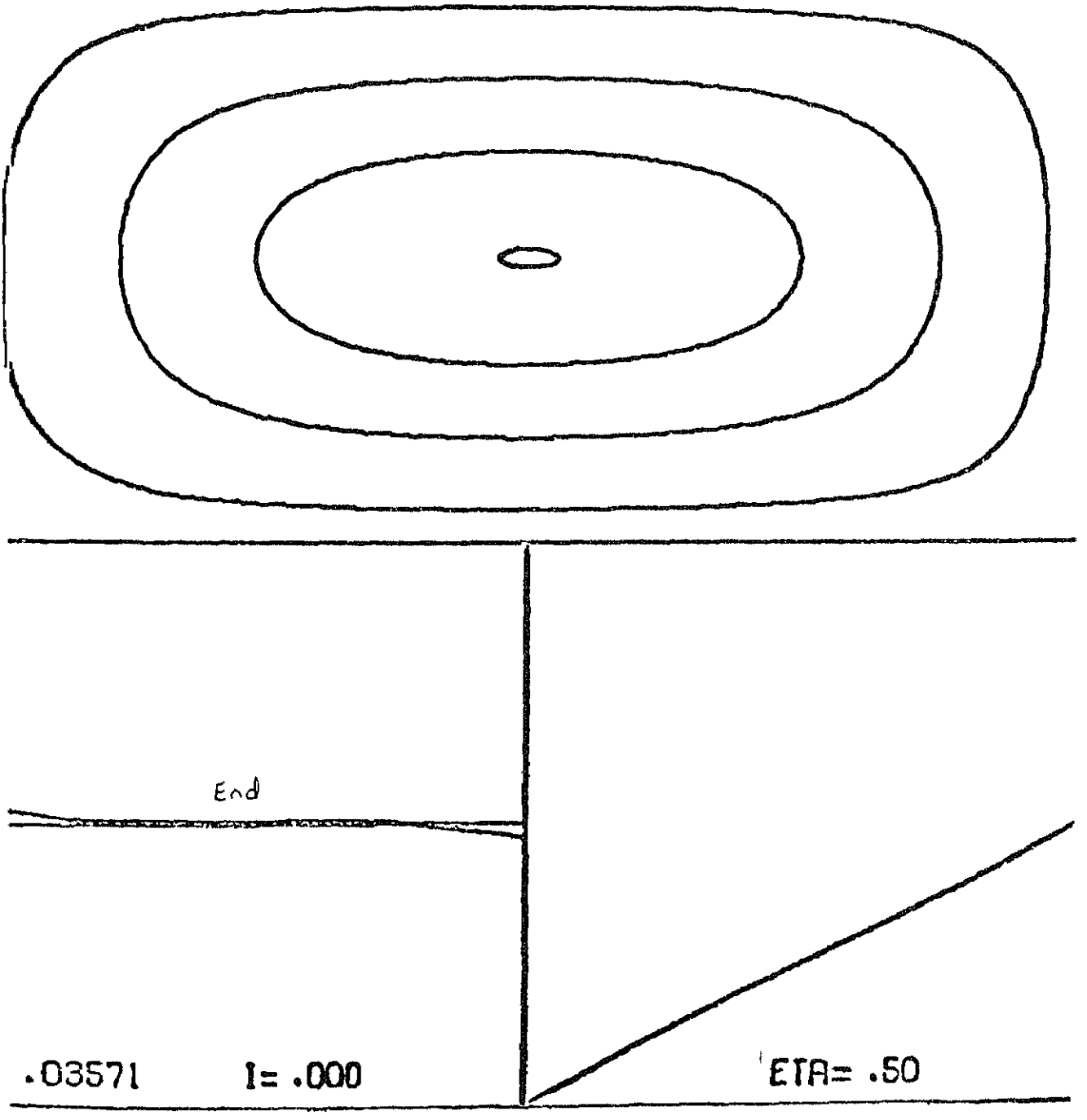
End
.03571
I= .000
ETA= .50

APPENDIX IV: TOKAMAK DATA REPORTING

We feel that it is essential that there be an improvement in the methods of data reporting. We recognize that all the important experimental data are not always available on every series of discharges. Our major concern is that the reduced data is often not available in an organized, standardized, and easily accessible form for widespread interlaboratory use in transport codes. There is an apparent lack of understanding in many cases as to what information is generally useful for this purpose.

In published experimental papers, the reduced data is often presented only in the context of analysis, interpretation, and experimental proof of a hypothesis. Thus only that part of the data thought to be relevant to the problem at hand gets reported. Information correlated on a shot-to-shot basis is not available in published papers. For example, it is of little use for transport code work to show "typical" profiles, time traces, or values of temperature uncorrelated with density, current, field, or working gas, etc. In many cases (e.g., scaling analysis), it is sufficient to report the "steady" parameters. Sometimes the ful' dynamic behavior is of interest (e.g., gas puffing t curves, information on whether or not the

We feel that understanding of results o generation of large devices will be dramatically improved if the large laboratory experiment (in particular, PLT, Alcator, ISX, and DIII) have

scientific "secretaries," as in the case of TFR, to collect and correlate the available reduced data in a standard form. What data should be reduced and in what form can only be decided by the experimentalists and interested theorists within the laboratory. This is already being done to some extent in each laboratory. The reduced data should be placed on the CTR network computer and made available to all interested workers. The time lag between data reduction and placement in the system should be sufficient to: (1) allow the data to "age" (i.e., until the experimentalists feel that it is reasonably correct), and (2) to allow some priority rights of the experimentalists to interpret the experiments "first." However, under the present conditions the time for data to become public is long compared to the time between major experiments.

Below we give some examples of data often available but not routinely reported in a correlated fashion.

1. Measurement of the radiation power loss density versus radius. Availability of this data is essential to understanding transport. If this quantity is significant relative to the total local power balance of the electrons, no treatment of the electron power balance can be given. It is insufficient to state the total power radiated; the discharge can be transport-dominated even when 100% of the power goes to radiation provided the central region has little radiation loss. Radiation (from high-Z impurities in particular) is uncorrelated

with any other parameter and because of its dependence on the surface source, it is a priori unpredictable in practice.

2. The neutral density at the center. In conjunction with standard charge exchange codes this data allows some inference on the plasma transport coefficient. The plasma transport relative to electron heat transport is an important signature of all transport theories. The neutral density at the center can be obtained from the absolute calibration of the charge exchange diagnostic which measures the ion temperatures.

In addition to making reduced working data available for transport code work, we feel that there is a need for more confinement scaling experiments on tokamaks. By scaling we simply mean a series of discharges under comparable machine conditions in which only one variable is changed. The reporting of "typical" discharges (frequently it means discharges having the maximum achievable confinement time) is of limited usefulness in transport codes since transport models will invariably have at least one adjustable parameter. As the tokamaks become cleaner (or if the radiation can be subtracted out as described above) and the shots become more reproducible, such experiments will take on added significance. Since we are limited to factors of 2 and 3 in many of the experimental parameters, fairly careful interpretation and analysis with transport codes is needed to correlate the data and account for profile changes due to radiation and MHD effects.

A community-wide review of this question is needed. A standards committee is needed which would establish reasonable guidelines for the dissemination of that data which never sees publication in finished form, but which is vital to detailed analysis of confinement processes. The predominant membership of this committee should be experimental.